CHAPTER

Band-Structure Calculations

5

CHAPTER OUTLINE

5.1 INTRODUCTION

In the preceding chapter, the nearly free electron approximation was described in detail. In this approximation, the valence electrons are considered to be nearly free electrons moving in a background of positive charges that are arranged in a regular array such that the potential is periodic. The positive charges are actually the cores of the atoms in which the valence electrons have been stripped from the parent atoms. These cores either are located at the lattice points or a group of cores is located symmetrically around each lattice point. The cores are constituted from atomic orbitals that are essentially localized. In general, these atomic orbitals do not overlap. However, in some cases, the localized atomic orbitals overlap to an extent such that they form Bloch functions in the crystalline solid.

5.2 TIGHT-BINDING APPROXIMATION

It is useful to formulate a linear combination of these atomic orbitals such that they would be Bloch functions as required for wave functions in a crystalline solid. Thus, the tight-binding approximation, formulated for the core electrons, complements the nearly free electron approximation formulated for

Physics of Condensed Matter. DOI: 10.1016/B978-0-12-384954-0.00005-0

the valence electrons. The tight-binding method is very useful in calculating the energy bands of partially filled *d*-shells of transition metal atoms as well as for describing the electronic structure of insulators.

In its simplest form, the tight-binding method can be expressed as follows. We assume that $\phi_a(\mathbf{r})$ is an atomic orbital for a free atom located at a lattice point at the origin; i.e., it is the ground state of an electron moving in the potential $v_a(\mathbf{r})$ of an isolated atom such that the energy is ε_a. As a first approximation, we consider a monatomic lattice with one atom located at each lattice point. We assume that the free atom is in an *s* state since the bands obtained from the other $(p, d, \ldots)$ states are much more complicated because the atomic levels are degenerate. We further assume that the influence of one atom on another is small. If the bound levels of the atomic Hamiltonian (H_a) are localized, the Schrodinger equation can be written as

$$H_a\phi_a(\mathbf{r}) = \varepsilon_a\phi_a(\mathbf{r}), \tag{5.1}$$

where

$$H_a = -\frac{\hbar^2}{2m}\nabla^2 + v_a. \tag{5.2}$$

The range of $\phi_a(\mathbf{r})$ is very small when $\mathbf{r}$ exceeds the distance of a lattice constant. However, in the crystalline solid, the Hamiltonian H would differ from the atomic Hamiltonian because of the corrections to the atomic potential in the crystal lattice. If we write $\Delta V(\mathbf{r})$ as the (small) correction to the atomic potential in the lattice (the difference between the periodic potential in the crystal lattice and the potential of an isolated atom), the crystal Hamiltonian H can be written as

$$H = H_a + \Delta V(\mathbf{r}). \tag{5.3}$$

The periodic potential $V(\mathbf{r})$ is the sum of the atomic potential $v_a(\mathbf{r})$ and the correction term $\Delta V(\mathbf{r})$,

$$V(\mathbf{r}) = v_a(\mathbf{r}) + \Delta V(\mathbf{r}). \tag{5.4}$$

In Figure 5.1, $r\phi_a(\mathbf{r})$ and $\Delta V(\mathbf{r})$ are drawn along a linear chain of the atomic sites that are located at the lattice points.

The Schrodinger equation can be written as

$$\left(\frac{-\hbar^2}{2m}\nabla^2 + V(\mathbf{r})\right)\psi_{\mathbf{k}}(\mathbf{r}) = E_{\mathbf{k}}\psi_{\mathbf{k}}(\mathbf{r}). \tag{5.5}$$

We note that the eigenfunctions $\psi_{\mathbf{k}}(\mathbf{r})$ have to be Bloch functions. As a zero-order approximation, we assume that $\Delta V(\mathbf{r}) = 0$ in the region where $\phi_a(\mathbf{r}) \neq 0$. In that case, we can construct the Bloch functions as a linear combination of the atomic orbitals

$$\psi_{\mathbf{k}}(\mathbf{r}) = \sum_i e^{i\mathbf{k}\cdot\mathbf{R}_i}\phi_a(\mathbf{r} - \mathbf{R}_i), \tag{5.6}$$

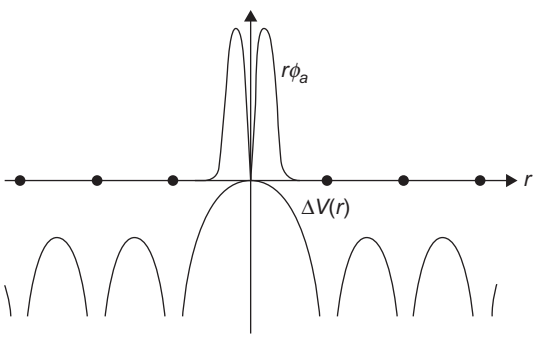

FIGURE 5.1

Here, $r\phi_a(\mathbf{r})$ and $\Delta V(\mathbf{r})$ are plotted against $\mathbf{r}$ in a linear chain of atomic sites.

where the $\mathbf{R}_i$ are the complete set of Bravais lattice vectors in the crystal lattice. We will now prove that $\psi_{\mathbf{k}}(\mathbf{r})$ are Bloch functions. From Eq. (5.6),

$$\begin{aligned}\psi_{\mathbf{k}}(\mathbf{r}+\mathbf{R}_j) &= \sum_i e^{i\mathbf{k}\cdot\mathbf{R}_i}\phi_a(\mathbf{r}+\mathbf{R}_j-\mathbf{R}_i)\\ &= e^{i\mathbf{k}\cdot\mathbf{R}_j}\sum_i e^{i\mathbf{k}\cdot(\mathbf{R}_i-\mathbf{R}_j)}\phi_a(\mathbf{r}+\mathbf{R}_j-\mathbf{R}_i)\\ &= e^{i\mathbf{k}\cdot\mathbf{R}_j}\sum_l e^{i\mathbf{k}\cdot\mathbf{R}_l}\phi_a(\mathbf{r}-\mathbf{R}_l)\\ &= e^{i\mathbf{k}\cdot\mathbf{R}_j}\psi_{\mathbf{k}}(\mathbf{r}),\end{aligned} \tag{5.7}$$

which are the criteria for the Bloch functions.

The expectation value of the energy can be written as

$$\varepsilon(\mathbf{k}) = \frac{\int \psi_{\mathbf{k}}^*\left[-\frac{\hbar^2}{2m}\nabla^2 + V(\mathbf{r})\right]\psi_{\mathbf{k}}(\mathbf{r})d\mathbf{r}}{\int \psi_{\mathbf{k}}^*(\mathbf{r})\psi_{\mathbf{k}}(\mathbf{r})d\mathbf{r}}. \tag{5.8}$$

Assuming that the overlap between the neighboring cells is small,

$$\int \psi_{\mathbf{k}}^*(\mathbf{r})\psi_{\mathbf{k}}(\mathbf{r})d\mathbf{r} \approx 1. \tag{5.9}$$

We obtain from Eqs. (5.4) and (5.8),

$$\varepsilon(\mathbf{k}) \approx \sum_{i,j} e^{i\mathbf{k}\cdot(\mathbf{R}_i-\mathbf{R}_j)}\int \phi_a^*(\mathbf{r}-\mathbf{R}_j)\left[-\frac{\hbar^2}{2m}\nabla^2 + v_a(\mathbf{r}) + \Delta V(\mathbf{r})\right]\phi_a(\mathbf{r}-\mathbf{R}_i)d\mathbf{r}. \tag{5.10}$$

From Eqs. (5.1) and (5.10), we can write $\varepsilon(\mathbf{k})$ in the alternate form

$$\varepsilon(\mathbf{k}) = \varepsilon_a + N\sum_l e^{-i\mathbf{k}\cdot\mathbf{R}_l}\int \phi_a(\mathbf{r}-\mathbf{R}_l)\Delta V(\mathbf{r})\phi_a(\mathbf{r})d\mathbf{r}. \tag{5.11}$$

Here, N is the number of atoms in the monatomic crystal lattice. Neglecting all integrals except those at the atomic sites and between the nearest-neighbor atomic sites and defining $\mathbf{R}_n$ as the nearest-neighbor lattice vectors of a primitive lattice in which the origin is located, we can rewrite Eq. (5.11) in the alternate form

$$\varepsilon(\mathbf{k}) \approx \varepsilon_a - \beta - \gamma\sum_l e^{-i\mathbf{k}\cdot\mathbf{R}_l}, \tag{5.12}$$

where

$$\beta = -N\int \phi_a^*(\mathbf{r})\Delta V(\mathbf{r})\phi_a(\mathbf{r})d\mathbf{r}, \tag{5.13}$$

and

$$\gamma = -N\int \phi_a^*(\mathbf{r}-\mathbf{R}_n)\Delta V(\mathbf{r})\phi_a(\mathbf{r})d\mathbf{r}. \tag{5.14}$$

As an example, we consider a simple cubic lattice. The nearest-neighbor positions of a simple cubic lattice of lattice constant a are $\mathbf{R}_n = (\pm a, 0, 0)$, and $(0, \pm a, 0)$, $(0, 0, \pm a)$. Thus, Eq. (5.12) becomes

$$\varepsilon(\mathbf{k}) = \varepsilon_a - \beta - 2\gamma(\cos k_x a + \cos k_y a + \cos k_z a). \tag{5.15}$$

The energies are located in a band of width 12 γ. If $ka \ll 1$, Eq. (5.15) yields

$$\varepsilon(\mathbf{k}) \cong \varepsilon_a - \beta - 6\gamma + \gamma k^2 a^2. \tag{5.16}$$

In this derivation, we have considered only one state (the s state) of the free atom and obtained one band. We note that usually for s states, $\beta = 0$. We also note that Eq. (5.15) is periodic in $\mathbf{k}$ and therefore only those values of $\mathbf{k}$ lying in the first Brillouin zone will define independent wave functions. The number of states in the first Brillouin zone that corresponds to a nondegenerate atomic level is equal to $2N$. In Figure 5.2, we schematically show $\varepsilon(\mathbf{k})$ plotted as a function of $\mathbf{k}$ along the cube axis by using the tight-binding method. Here, $\varepsilon(\mathbf{k})$ has a minimum at $\mathbf{k} = 0$ along the cube direction and a maximum at $\mathbf{k} = (\pi/a, 0, 0)$, which is the zone boundary.

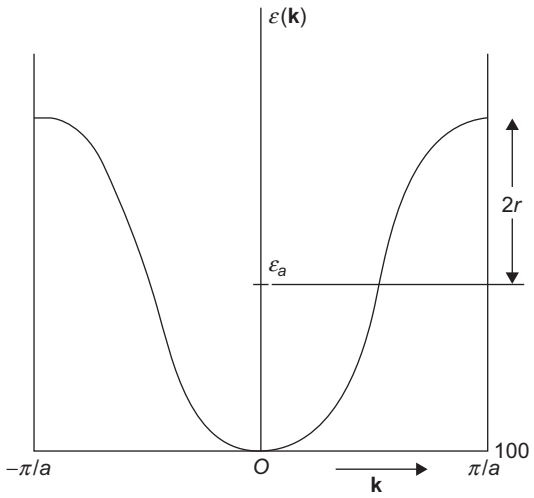

FIGURE 5.2

Here, $\varepsilon(\mathbf{k})$ is plotted as a function of $\mathbf{k}$ along the cube axis.

Thus, for every state of an electron in the free atom, there will be a band of energies in the crystal. The complexities of the problem increase for higher atomic levels. One can generalize by stating that when N identical atoms are kept far apart, and each atom has several different atomic levels (orbitals), there will be N-fold degenerate states for a single electron. When these atoms are brought closer, the atomic orbitals overlap, and a band that has N states is formed. This is shown in Figure 5.3.

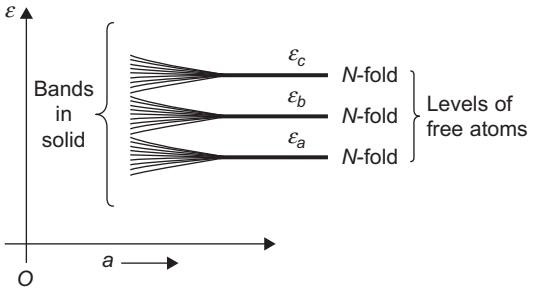

FIGURE 5.3

Formation of bands from atomic levels as the atoms come closer.

Thus, one can refer to the 3s-band, 3p-band, 3d-band, and so on. It is too simplistic to consider these higher atomic states in the simple tight-binding method discussed previously. However, in Figure 5.3, we have schematically shown the formation of bands in solids by using the tight-binding method. Figure 5.4 shows the broadening of the bands that ultimately overlap.

It is important to note at this stage that when these bands, formed from different atomic orbitals, broaden and overlap, the tight-binding method has to be modified and one uses the linear combination of atomic orbitals (LCAO method). We will discuss specific cases of such overlaps when we consider the p- and d-bands as well as the s-d "resonance" bands.

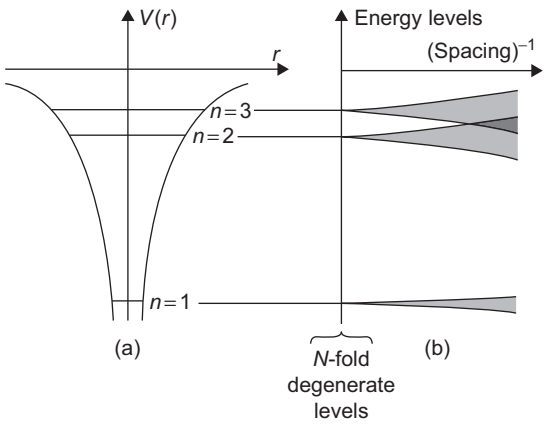

FIGURE 5.4

(a) Nondegenerate atomic levels; (b) energy levels of N such atoms in a periodic array plotted as a function of mean interatomic spacing.

5.3 LCAO METHOD

In the linear combination of atomic orbitals (LCAO) method (Ref. 18), the Bloch wave function of the crystalline solid is expanded in terms that are linear combinations of atomic orbitals. Thus, Eq. (5.1) is rewritten as

$$\psi_{\mathbf{k}}(\mathbf{r}) = \sum_i e^{i\mathbf{k}\cdot\mathbf{R}_i}\phi_c(\mathbf{r}-\mathbf{R}_i), \tag{5.17}$$

where

$$\phi_c(\mathbf{r}) = \sum_j \beta_j \phi_j(\mathbf{r}), \tag{5.18}$$

β_j are arbitrary constants to be determined, and $\phi_j(\mathbf{r})$ is one of the set of localized atomic orbitals on the atom located at the origin. In general, $\psi_{\mathbf{k}}(\mathbf{r})$ is used as a trial wave function and β_j are obtained by minimizing the ground-state energy.

The crystal Schrodinger equation can be rewritten as

$$H\psi_{\mathbf{k}}(\mathbf{r}) = \varepsilon(\mathbf{k})\psi_{\mathbf{k}}(\mathbf{r}), \tag{5.19}$$

where

$$H = H_{at} + \Delta V(\mathbf{r}). \tag{5.20}$$

Multiplying Eq. (5.19) by one of the atomic wave functions, $\phi_a{}^*(\mathbf{r})$, and integrating over all $\mathbf{r}$, we obtain

$$\int \phi_a{}^*(\mathbf{r})[H_{at} + \Delta V(\mathbf{r})]\psi_{\mathbf{k}}(\mathbf{r})d\mathbf{r} = \varepsilon(\mathbf{k})\int \phi_a{}^*(\mathbf{r})\psi_{\mathbf{k}}(\mathbf{r})d\mathbf{r}, \tag{5.21}$$

which can be rewritten in the alternate form

$$(\varepsilon(\mathbf{k})-\varepsilon_a)\int \phi_a{}^*(\mathbf{r})\psi_{\mathbf{k}}(\mathbf{r})d\mathbf{r} = \int \phi_a{}^*(\mathbf{r})\Delta V(\mathbf{r})\psi_{\mathbf{k}}(\mathbf{r})d\mathbf{r}, \tag{5.22}$$

where we have used Eq. (5.1) to obtain ε_a. Because the atomic orbitals are orthonormal, i.e.,

$$\int \phi_a{}^*(\mathbf{r})\phi_{a'}(\mathbf{r})d\mathbf{r} = \delta_{aa'}, \tag{5.23}$$

we obtain from Eqs. (5.17), (5.18), and (5.23),

$$\int \phi_a{}^*(\mathbf{r})\psi_{\mathbf{k}}(\mathbf{r})d\mathbf{r} = \beta_a + \sum_j \beta_j \left(\sum_{i\neq 0} \int \phi_a{}^*(\mathbf{r})\phi_j(\mathbf{r}-\mathbf{R}_i)e^{i\mathbf{k}\cdot\mathbf{R}_i}d\mathbf{r} \right). \tag{5.24}$$

From Eqs. (5.21), (5.23), and (5.24), we obtain

$$\begin{aligned}\Big(\varepsilon(\mathbf{k})-\varepsilon_a\Big)\beta_a = (\varepsilon_a - \varepsilon(\mathbf{k})\sum_j \beta_j \left(\sum_{i\neq 0} \int \phi_a{}^*(\mathbf{r})\phi_j(\mathbf{r}-\mathbf{R}_i)e^{i\mathbf{k}\cdot\mathbf{R}_i}d\mathbf{r} \right) \\ + \sum_j \beta_j \left(\int \phi_a{}^*(\mathbf{r})\Delta V(\mathbf{r})\phi_j(\mathbf{r})d\mathbf{r} \right) \\ + \sum_j \beta_j \left(\sum_{i\neq 0} \int \phi_a{}^*(\mathbf{r})\Delta V(\mathbf{r})\phi_j(\mathbf{r}-\mathbf{R}_i)e^{i\mathbf{k}\cdot\mathbf{R}_i}d\mathbf{r} \right).\end{aligned} \tag{5.25}$$

We note that each of the three terms on the right side of the equation is small (for different reasons) unless the atomic levels are degenerate. The first term contains the overlap integrals $\int \phi_a{}^*(\mathbf{r})\phi_j(\mathbf{r}-\mathbf{R}_i)d\mathbf{r}$ where $\mathbf{R}_i \neq 0$. The atomic wave functions are centered on different lattice sites, and therefore, the overlap is very small compared to unity because the atomic orbitals are well localized. The second term on the right side of the equation is small because at large distances, where $\Delta V(\mathbf{r})$ (which is the difference between the periodic and atomic potentials) is significant, the atomic wave functions are small. The third term on the right side is small for the same reason as the first term, because they also contain atomic wave functions centered at different sites.

If the atomic levels are nondegenerate, i.e., for an *s*-level, Eq. (5.25) is essentially the same as Eq. (5.13). For bands arising from atomic *p*-levels, which are triple-degenerate, Eq. (5.25) would give a set of three homogeneous equations. One has to solve a 3×3 secular problem. The eigenvalues would give $\varepsilon(\mathbf{k})$ for the three bands, and $\beta(\mathbf{k})$, the appropriate linear combination of the atomic orbitals at the various $\mathbf{k}$ values in the Brillouin zone, would be obtained from the solutions. Similarly, the *d*-levels are five-fold degenerate and yield five homogeneous equations. One has to solve a 5×5 problem to obtain the eigenvalues as well as the values of $\beta(\mathbf{k})$. In transition metals, the *s* and *d* electrons overlap in energy. In addition, because the *s* electrons have a large degree of plane wave character, they have essentially a uniform spatial distribution. Therefore, there is a spatial overlap between the *s* and the *d* orbitals. There is an intra-atomic *s*-*d* resonance that hybridizes the *s*- and *d*-bands due to this overlap in both real space and energy. Therefore, for transition metals, one has to solve a 6×6 secular problem that includes both *d*- and *s*-levels.

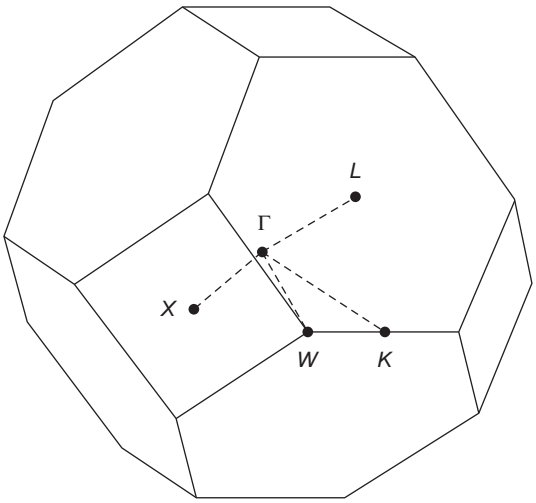

FIGURE 5.5

ΓX direction of the first Brillouin zone of the fcc structure.

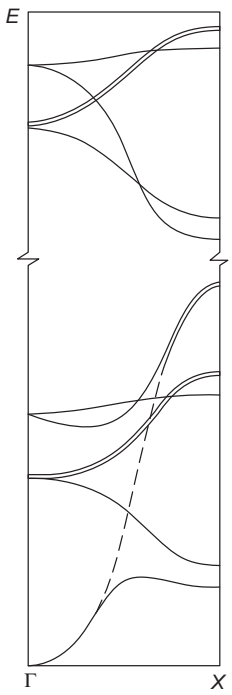

FIGURE 5.6

The five *d* sub-bands of a transition metal atom in the ΓX direction of a fcc structure.

The five *d* sub-bands of a transition metal in the ΓX direction in the fcc structure that is shown in Figure 5.5 are shown in Figure 5.6.

The progression of the 3*d*-band through the Fermi energy for elements in and near the long series of transition metals is shown in Figure 5.7. The bands that are primarily of *sp* character are shown by the heavier lines.

The tight-binding approximation is more complicated in crystalline solids in which the Bravais lattice is not monatomic. For example, the hexagonal close-packed metals are simple hexagonal with a two-point basis. There are two ways of solving this problem. One procedure is to consider the two-point basis as a molecule, of which the wave functions are known, and treat the problem in the same manner as we have done for a monatomic lattice, except that in this case, molecular wave functions are used instead of atomic wave functions. For *s*-levels, for which the nearest-neighbor overlaps are small, the overlap would be small in the molecule. Thus, an atomic *s*-level will give rise to two nearly degenerate molecular levels and hence will yield two tight-binding bands. The alternate

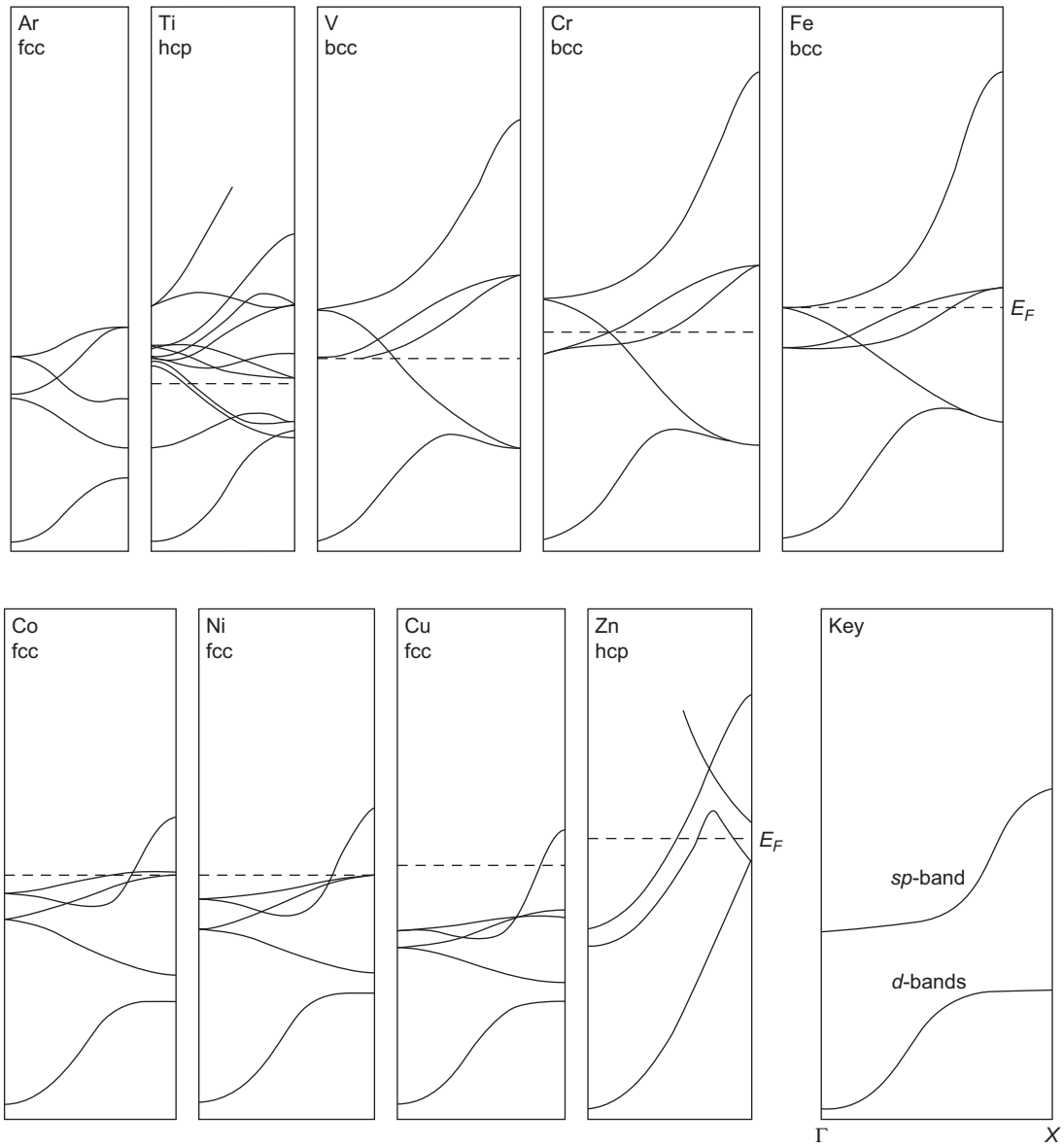

FIGURE 5.7

The progression of the 3*d*-band through the Fermi energy for elements in and near the first long series of transition metals.

method is to make linear combinations of atomic levels centered at the Bravais lattice points and at the basis points. The LCAO wave function would be of the form

$$\psi_{\mathbf{k}}(\mathbf{r}) = \sum_i \Big(a_1\phi(\mathbf{r}-\mathbf{R}_i) + a_2\phi(\mathbf{r}-\mathbf{R}_i+\mathbf{l})\Big)e^{i\mathbf{k}\cdot\mathbf{R}_i}, \tag{5.26}$$

where $\mathbf{l}$ is the vector connecting the two basis atoms in the Bravais lattice.

In these methods of tight-binding calculations, we have considered only the spin-independent linear combinations of atomic orbitals, thereby implicitly neglecting spin-orbit coupling, which is important in calculating the atomic levels in the heavier elements. We can include spin-orbit coupling by considering the interaction of the electron spin on the orbital of its parent atom located at the origin as well as by including the interaction between the spin of that electron and the electric field of all the other ions in $\Delta V(\mathbf{r})$. In this method, we must use linear combinations of the spin-dependent atomic wave functions.

The LCAO method is not very satisfactory for the quantitative calculation of Bloch functions in solids. It is very difficult to calculate the three-center integrals and nonorthogonal basis functions. In addition, representing the valence electron states in a metal or a semiconductor by an expression such as Eq. (5.17) is basically wrong. We consider the interstitial region, the creation of which is illustrated in Figures 5.8 and 5.9. Figure 5.8 shows the bound atomic orbitals of two free atoms.

In Figure 5.9, these two bound atomic orbitals are superposed, thereby creating an interstitial region with a small constant potential.

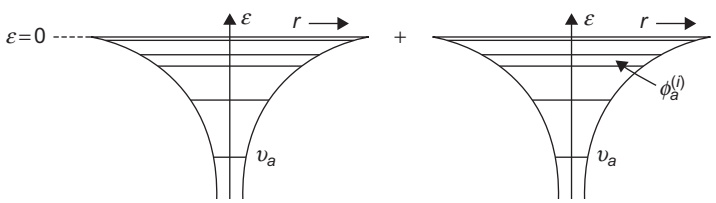

FIGURE 5.8

Potential wells centered on the nuclei of two free atoms.

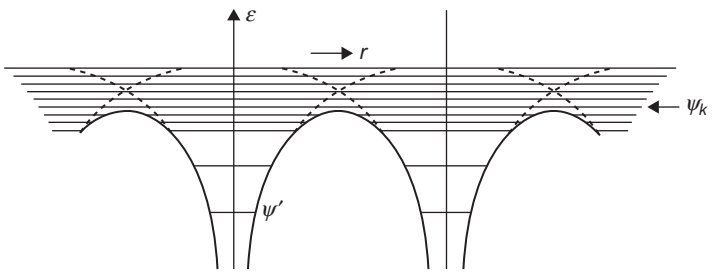

FIGURE 5.9

The Bloch functions in a crystalline lattice.

The individual atomic orbitals, used in Eq. (5.17), do not exist in the interstitial regions between the main potential wells centered on the atomic nuclei because they would lie above the energy of the barriers between the atomic spheres. It is also inappropriate to represent a Bloch function, which is a consequence of a periodic potential $V(\mathbf{r})$ in the crystalline solid, by a linear combination of the atomic orbitals $\phi_a(\mathbf{r})$, which arise due to an atomic potential $v_a(\mathbf{r})$ and rapidly tend to zero as $\mathbf{r}\rightarrow\infty$.

Finally, the set of functions used in the LCAO method is incomplete because it does not include the scattered-wave eigenstates in the Schrodinger equation in the continuum, above the energy zero of $v_a(\mathbf{r})$. They are useful in the construction of the Bloch functions inside the atomic core but inappropriate in the interstitial region, where the use of a linear combination of plane waves is more appropriate.

The main disadvantage of the tight-binding as well as the LCAO methods is that the independent electron approximation is one of the bases of these approximations. This approximation works very well for both insulators and the low-lying bands in metals. In such cases, the tight-binding bands are very low in energy and completely filled. However, the independent electron approximation in the formulation of the tight-binding method fails when there are partially filled bands that are obtained from localized atomic orbitals with small overlap integrals. In particular, when we consider the properties of the narrow tight-binding bands that are obtained from partially filled atomic shells, the failure of the independent electron approximation becomes more apparent and leads to anomalous results. When one uses the tight-binding method for the d- and f-shells in metals, the inclusion of the electron–electron interaction becomes very important. In particular, when there is a magnetic structure, this failure is even more apparent.

One of the important reasons for going beyond the tight-binding approximation is that when there is a second electron at a given atomic site, the strong repulsion between the first electron and the second electron at the same site cannot be treated by the independent electron approximation.

An interesting consequence of the tight-binding approximation is the hypothetical question as to what would happen if the distance between the atoms is continuously increased so that there is a slow but steady transition from the metallic to the atomic state. The overlap integrals would become smaller with the increase of the lattice constant, and eventually all bands, including the partially filled conduction band(s), become very narrow tight-binding bands. The decrease of electrical conductivity of a metal would continuously drop with the decrease of the overlap integrals as the lattice constant increases and eventually would become zero. Thus, the metal would become an insulator. This is known as a Mott transition. In practice, if electron–electron interactions are included, the conductivity would abruptly become zero at a Mott transition.

The Mott transition has indeed been observed in certain transition metal oxides. They are normally insulators but suddenly become good conductors above a certain temperature.

5.4 WANNIER FUNCTIONS

One of the main problems of the tight-binding formulation is caused by the difficulties of orthogonalization since a linear combination of the atomic orbitals is used. This orthogonalization problem can be circumvented by defining a set of orthonormal wave functions that can be constructed from Bloch functions and are localized on the atomic sites. These functions are known as Wannier functions. The Wannier function (Ref. 19) centered at the lattice site $\mathbf{R}_i$ is defined as

$$w_n(\mathbf{r}-\mathbf{R}_i) = \frac{1}{\sqrt{N}}\sum_{\mathbf{k}} e^{-i\mathbf{k}\cdot\mathbf{R}_i}\psi_{n\mathbf{k}}(\mathbf{r}), \tag{5.27}$$

where N is the number of lattice sites as well as the number of $\mathbf{k}$ states in the first Brillouin zone. We will now show that the Wannier functions form an orthonormal set:

$$\int d\mathbf{r}\, w_m^*(\mathbf{r}-\mathbf{R}_j) w_n(\mathbf{r}-\mathbf{R}_i) = \int d\mathbf{r} \sum_{\mathbf{k}} \sum_{\mathbf{k}'} \frac{1}{N} e^{-i\mathbf{k}\cdot\mathbf{R}_i + i\mathbf{k}'\cdot\mathbf{R}_j} \psi_{m\mathbf{k}'}^*(\mathbf{r}) \psi_{n\mathbf{k}}(\mathbf{r}). \tag{5.28}$$

Because the Bloch functions are orthonormal (Problem 5.3), i.e.,

$$\int d\mathbf{r}\, \psi_{m\mathbf{k}'}^*(\mathbf{r}) \psi_{n\mathbf{k}}(\mathbf{r}) d\mathbf{r} = \delta_{m,n}\delta_{\mathbf{k},\mathbf{k}'}, \tag{5.29}$$

Eq. (5.28) can be rewritten in the alternate form

$$\int d\mathbf{r}\, w_m^*(\mathbf{r}-\mathbf{R}_j) w_n(\mathbf{r}-\mathbf{R}_i) = \frac{1}{N} \sum_{\mathbf{k}} \sum_{\mathbf{k}'} e^{-i\mathbf{k}\cdot\mathbf{R}_i + i\mathbf{k}'\cdot\mathbf{R}_j} \delta_{m,n}\delta_{\mathbf{k},\mathbf{k}'}. \tag{5.30}$$

Because it can be easily shown that (Problem 5.4)

$$\sum_{\mathbf{k}} e^{-i\mathbf{k}\cdot(\mathbf{R}_i - \mathbf{R}_j)} = N\delta_{i,j}, \tag{5.31}$$

we obtain from Eqs. (5.30) and (5.31) the orthonormal conditions of the Wannier functions,

$$\int d\mathbf{r}\, w_m^*(\mathbf{r}-\mathbf{R}_j) w_n(\mathbf{r}-\mathbf{R}_i) = \delta_{m,n}\delta_{i,j}. \tag{5.32}$$

If the Wannier functions are known, one can obtain the Bloch functions from Eq. (5.27) by multiplying both sides by $e^{i\mathbf{k}'\cdot\mathbf{R}_i}$ and summing over all direct lattice vectors $\mathbf{R}_i$,

$$\sum_{\mathbf{R}_i} e^{i\mathbf{k}'\cdot\mathbf{R}_i} w_n(\mathbf{r}-\mathbf{R}_i) = \frac{1}{\sqrt{N}} \sum_{\mathbf{R}_i} \sum_{\mathbf{k}} e^{-i(\mathbf{k}-\mathbf{k}')\cdot\mathbf{R}_i} \psi_{n\mathbf{k}}(\mathbf{r}). \tag{5.33}$$

It can be easily shown that (Problem 5.5)

$$\sum_{\mathbf{R}_i} e^{-(\mathbf{k}-\mathbf{k}')\cdot\mathbf{R}_i} = N\delta_{\mathbf{k},\mathbf{k}'}. \tag{5.34}$$

From Eqs. (5.33) and (5.34), we obtain

$$\psi_{n\mathbf{k}}(\mathbf{r}) = \frac{1}{\sqrt{N}} \sum_{\mathbf{R}_i} e^{i\mathbf{k}\cdot\mathbf{R}_i} w_n(\mathbf{r}-\mathbf{R}_i). \tag{5.35}$$

It may be noted that any Bloch function is determined only within an overall phase factor. So the Wannier functions defined in Eq. (5.27) can also be defined as

$$w_n(\mathbf{r}-\mathbf{R}_i) = \frac{1}{\sqrt{N}} \sum_{\mathbf{k}} e^{-i\mathbf{k}\cdot\mathbf{R}_i + i\varphi(\mathbf{k})} \psi_{n\mathbf{k}}(\mathbf{r}), \tag{5.36}$$

where $\varphi(\mathbf{k})$ is an arbitrary real function. The Wannier functions can be optimized by making them drop off as fast as possible when $\mathbf{r}-\mathbf{R}_i$ starts increasing. This can be achieved by manipulating the arbitrary function $\varphi(\mathbf{k})$. The Wannier functions on adjacent sites can be schematically shown as in Figure 5.10.

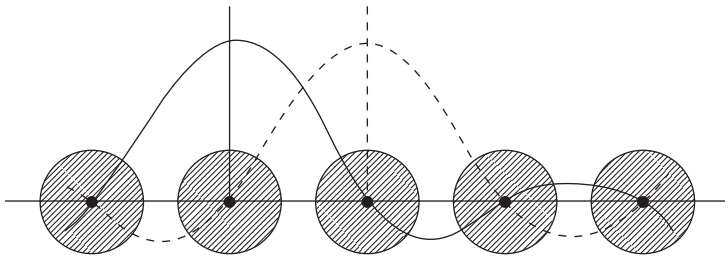

FIGURE 5.10

The Wannier functions on adjacent sites.

5.5 CELLULAR METHOD

The cellular method was originally proposed by Wigner and Seitz (Ref. 20) to calculate the band structure of sodium. Later, with the availability of powerful computers that could solve differential equations, the cellular method was considerably improved and generalized to calculate the band structure of metals. The essential principle behind the cellular method is that because of the Bloch condition

$$\psi_{\mathbf{k}}(\mathbf{r}+\mathbf{R}_i) = e^{i\mathbf{k}\cdot\mathbf{R}_i}\psi_{\mathbf{k}}(\mathbf{r}), \tag{5.37}$$

it is sufficient to solve the Schrodinger equation in Eq. (5.5) within a single primitive cell C. The wave function in other primitive cells can be obtained from its values in C by using Eq. (5.37). However, both $\psi_{\mathbf{k}}(\mathbf{r})$ and $\nabla\psi_{\mathbf{k}}(\mathbf{r})$ must be continuous as $\mathbf{r}$ crosses the cell boundary.

In the original Wigner–Seitz formulation, the Wigner–Seitz cell of a fcc or a bcc lattice is a polyhedron (see Figure 5.11) that could be approximated as a sphere of equal volume of which the radius is r_s. We will denote this sphere as the Wigner–Seitz sphere.

In addition, they considered the lowest state energy of sodium metal so that $\mathbf{k}=0$. Thus, the boundary conditions reduce to

$$\psi_{\mathbf{k}}(\mathbf{r}+\mathbf{R}_i) = \psi_{\mathbf{k}}(\mathbf{r}), \tag{5.38}$$

and because $\psi_{\mathbf{k}}(\mathbf{r})$ is periodic from cell to cell, it should have a horizontal tangent at the surface of the Wigner–Seitz sphere

$$\left[\frac{\partial\psi_{\mathbf{k}}}{\partial\mathbf{r}}\right]_{r=r_s} = 0. \tag{5.39}$$

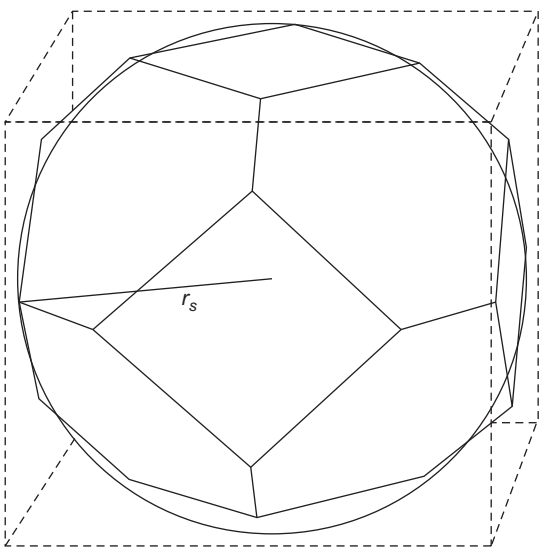

FIGURE 5.11

Wigner–Seitz cell of sodium metal (bcc structure) approximated as a sphere.

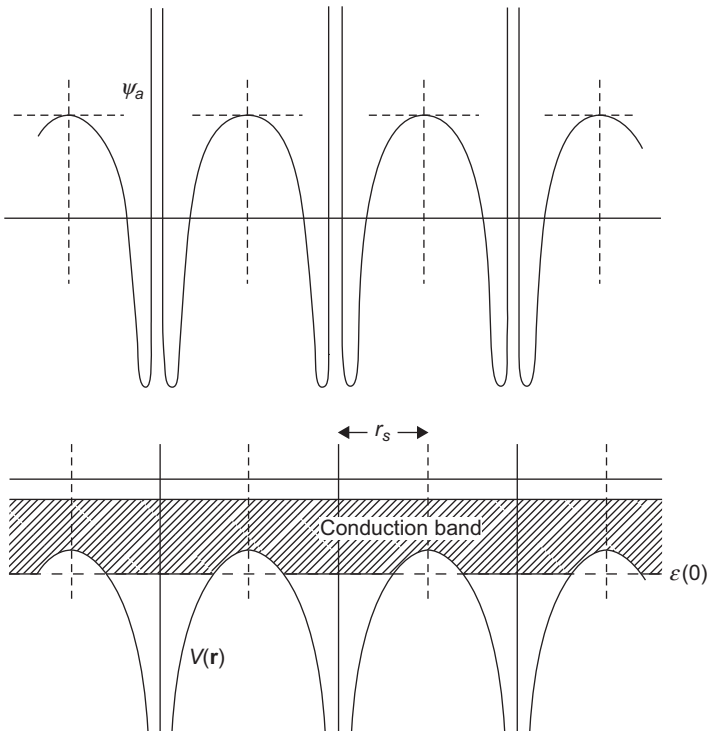

FIGURE 5.12

The ground-state energy $\varepsilon(0)$ of sodium metal in the Wigner–Seitz method.

For a potential that is symmetric inside the sphere, the energy $\varepsilon(0)$ can be defined as shown in Figure 5.12.

One can also write, by using the Bloch condition,

$$\psi_{\mathbf{k}}(\mathbf{r}) = e^{i\mathbf{k}\cdot\mathbf{r}} u_{\mathbf{k}}(\mathbf{r}), \tag{5.40}$$

where $u_{\mathbf{k}}(\mathbf{r})$ is the periodic part of the Bloch function. From Eqs. (5.5) and (5.40),

$$-\frac{\hbar^2}{2m}(\nabla^2 + 2i\mathbf{k}\cdot\nabla - k^2)u_{\mathbf{k}}(\mathbf{r}) + V(\mathbf{r})u_{\mathbf{k}}(\mathbf{r}) = \varepsilon(\mathbf{k})u_{\mathbf{k}}(\mathbf{r}), \tag{5.41}$$

where $u_{\mathbf{k}}(\mathbf{r})$ has a horizontal tangent at $r = r_s$. The shape of the band can be approximately obtained by using this method. However, the structure of the solid is neglected in this procedure.

There has been considerable improvement in the techniques of the cellular method for calculation of the band structure since Wigner and Seitz's original papers in 1933 and 1934 (Ref. 21). The starting point is the boundary conditions that $\psi_{\mathbf{k}}(\mathbf{r})$ *and* $\nabla\psi_{\mathbf{k}}(\mathbf{r})$ must be continuous as $\mathbf{r}$ crosses the boundary of the primitive cell C (usually located at the origin, i.e., $\mathbf{R} = 0$) to the neighboring cell

located at the lattice point $\mathbf{R}$. These boundary conditions, which introduce the wave vector $\mathbf{k}$ in the solution as well as retain the discrete set of energies $\varepsilon_n(\mathbf{k}) = \varepsilon$, can be restated as

$$\psi_{\mathbf{k}}(\mathbf{r}) = e^{-i\mathbf{k}\cdot\mathbf{R}}\psi_{\mathbf{k}}(\mathbf{r}+\mathbf{R}) \tag{5.42}$$

and

$$\nabla\psi_{\mathbf{k}}(\mathbf{r}) = e^{-i\mathbf{k}\cdot\mathbf{R}}\nabla\psi_{\mathbf{k}}(\mathbf{r}+\mathbf{R}) \tag{5.43}$$

for pairs of points on the surface separated by $\mathbf{R}$. If the point $\mathbf{r}$ is located on the surface of the primitive cell C, the normals $\hat{\mathbf{n}}$ to surface of the cell at $\mathbf{r}$ and $\mathbf{r}+\mathbf{R}$ are oppositely directed. Therefore, the continuity condition (Eq. 5.43) can be rewritten as (Problem 5.7)

$$\hat{\mathbf{n}}(\mathbf{r})\cdot\nabla\psi_{\mathbf{k}}(\mathbf{r}) = -e^{-i\mathbf{k}\cdot\mathbf{R}}\hat{\mathbf{n}}(\mathbf{r}+\mathbf{R})\cdot\nabla\psi_{\mathbf{k}}(\mathbf{r}+\mathbf{R}). \tag{5.44}$$

In the cellular method, the periodic potential $V(\mathbf{r})$ in the Wigner–Seitz cell C (see Figure 5.13) is replaced by a potential $V'(\mathbf{r})$ that has spherical symmetry (see Figure 5.14) about the origin.

Because we have made the approximation that the potential $V'(\mathbf{r})$ is spherically symmetric inside the cell C, a complete set of solutions to the Schrodinger equation (Eq. 5.5) is of the form (see Goswami[7] or any book on quantum mechanics)

$$\psi_{\varepsilon lm}(\mathbf{r}) = R_{\varepsilon l}(r)Y_{lm}(\theta,\phi), \tag{5.45}$$

where $Y_{lm}(\theta,\phi)$ are the spherical harmonics and $R_{\varepsilon l}(r)$ satisfies the differential equation

$$\left[\frac{1}{r^2}\frac{d}{dr}(r^2\frac{d}{dr}) + \frac{2m}{\hbar^2}\left(\varepsilon - V'(r) - \frac{\hbar^2 l(l+1)}{2mr^2}\right)\right]R_{\varepsilon l}(r) = 0. \tag{5.46}$$

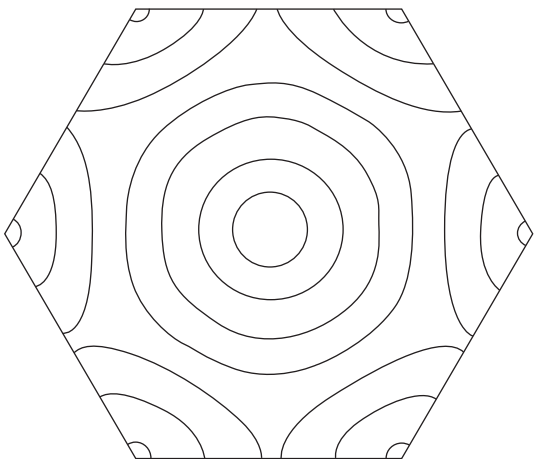

FIGURE 5.13
The actual potential $V(\mathbf{r})$ inside a primitive cell.

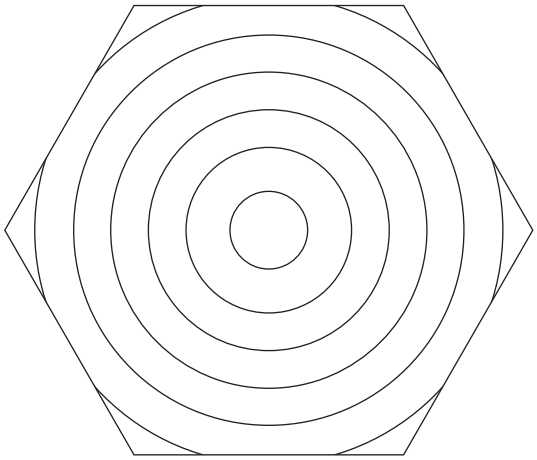

FIGURE 5.14
The approximate potential $V'(\mathbf{r})$ with spherical symmetry.

Here, we have written ε instead of n (which is appropriate for an atom) for the quantum number related to energy. Any linear combination of Eq. (5.45) would also be a solution of Eq. (5.5). Thus, we obtain

$$\psi(\mathbf{r}, \varepsilon) = \sum_{lm} B_{lm} R_{\varepsilon l}(r) Y_{lm}(\theta, \phi), \tag{5.47}$$

where the arbitrary coefficients B_{lm} are determined from the boundary conditions in Eqs. (5.42) and (5.44). In actual computations, a finite number of B_{lm} are chosen, and an equal number of points on the surface of the cell are chosen where the boundary conditions in Eqs. (5.42) and (5.44) are imposed. One obtains a set of $\mathbf{k}$-dependent linear homogeneous equations for B_{lm}. The energies $\varepsilon_n(\mathbf{k})$ are those values of ε for which the determinant of the homogeneous equations for B_{lm} vanishes.

5.6 ORTHOGONALIZED PLANE-WAVE (OPW) METHOD

The nearly free electron method does not account for the rapid oscillatory behavior in the core region of the atom. On the other hand, the tight-binding method, which matches reasonably well to $\psi_{\mathbf{k}}(\mathbf{r})$ inside the atomic core, does not account for the scattered-wave eigenstates of the Schrodinger equation in the continuum above the energy zero of the atomic potential $v_a(\mathbf{r})$. The Bloch states in the interstitial region must behave like a combination of free electron plane wave states. This anomaly of finding a complete set of wave functions that can account for the entire region in the crystal was resolved by the orthogonalized plane-wave (OPW) method first introduced by Herring. This method is based on the basic fact that the eigenfunctions of the crystalline Hamiltonian must be orthogonal at every point in the crystal.

In the OPW method, one starts with the construction of a complete set of Bloch functions for the core states. Here, the core states are defined as the atomic orbitals of the ions. A tight-binding combination of the core states, which are Bloch functions, as constructed in Eq. (5.17), can be written as

$$\phi_{c\mathbf{k}}(\mathbf{r}) = \sum_{\mathbf{R}_i} e^{i\mathbf{k}\cdot\mathbf{R}_i} \phi_c(\mathbf{r} - \mathbf{R}_i), \tag{5.48}$$

where $\phi_c(\mathbf{r})$ is one of the core orbital c. Here, the core wave functions are localized around the atomic sites and are assumed to be known. In fact, $\phi_c(\mathbf{k})$ is a linear combination of degenerate one-electron states. Thus, Eq. (5.48) is one of the solutions of the Schrodinger equation of the crystal with energy $\varepsilon_c(\mathbf{k})$. As we have noted in the discussion of the tight-binding method, this would form a fully occupied narrow band.

If we denote $\chi_{\mathbf{k}}(\mathbf{r})$ as a wave function for one of the higher states, it should be orthogonal to the core states defined in Eq. (5.48). In addition, the higher states $\chi_{\mathbf{k}}(\mathbf{r})$ must have the properties of a free electron wave function (plane wave)$e^{i\mathbf{k}\cdot\mathbf{r}}$ in the interstitial region. Thus, we can define the OPW as

$$\chi_{\mathbf{k}}(\mathbf{r}) = e^{i\mathbf{k}\cdot\mathbf{r}} - \sum_c b_c \phi_{c\mathbf{k}}(\mathbf{r}), \tag{5.49}$$

where the sum is over all the core levels. The coefficients b_c are determined from the orthogonalization condition

$$\int d\mathbf{r}\, \phi^*_{c\mathbf{k}}(\mathbf{r})\chi_{\mathbf{k}}(\mathbf{r}) = 0. \tag{5.50}$$

From Eqs. (5.49) and (5.50), we obtain

$$b_c = \int d\mathbf{r}\, \phi^*_{c\mathbf{k}}(\mathbf{r})e^{i\mathbf{k}\cdot\mathbf{r}}. \tag{5.51}$$

In deriving Eq. (5.51), we have made the basic assumption that the core states are orthogonal, i.e.,

$$\int d\mathbf{r}\, \phi^*_{c\mathbf{k}}(\mathbf{r})\phi_{c'\mathbf{k}}(\mathbf{r}) = \delta_{c,c'}. \tag{5.52}$$

The OPW state $\chi_{\mathbf{k}}(\mathbf{r})$ defined in Eq. (5.49) is appropriate for the interstitial region because the core states are localized, and consequently, each $\phi_{c\mathbf{k}}$ is small. Thus, $\chi_{\mathbf{k}}(\mathbf{r})$ behaves like the plane wave $e^{i\mathbf{k}\cdot\mathbf{r}}$ in the interstitial region. However, because $\chi_{\mathbf{k}}(\mathbf{r})$ is orthogonal to the core state within the core, it is appropriately a higher atomic orbital than the occupied atomic states. For example, if the core states are $2s$ and $2p$ orbitals, $\chi_{\mathbf{k}}(\mathbf{r})$ will behave like a $3s$ or $3p$ orbital with an extra nodal surface.

A schematic representation of an OPW is shown in Figure 5.15.

The eigenfunctions of the Schrodinger equation in the crystalline lattice can be expressed as a linear combination of OPWs that would form the basis states. The wave function can be written as

$$\psi_{\mathbf{k}}(\mathbf{r}) = \sum_{\mathbf{K}} C_{\mathbf{k}-\mathbf{K}}\chi_{\mathbf{k}-\mathbf{K}}(\mathbf{r}). \tag{5.53}$$

The coefficients $C_{\mathbf{k}-\mathbf{K}}$ are obtained by using the variational principle, to minimize the expectation value of the energy. The variational principle is briefly explained here.

If we define the energy functional

$$\varepsilon[\phi] = \frac{\int\left(\frac{\hbar^2}{2m}\,|\,\nabla\phi(\mathbf{r})\,|^2 + V(\mathbf{r})\,|\,\phi(\mathbf{r})\,|^2\right)d\mathbf{r}}{\int|\phi(\mathbf{r})|^2 d\mathbf{r}}, \tag{5.54}$$

it follows from Eq. (11) of Problem 5.8 that

$$\varepsilon[\psi_{\mathbf{k}}] = \varepsilon_{\mathbf{k}}, \tag{5.55}$$

which is the variational principle.

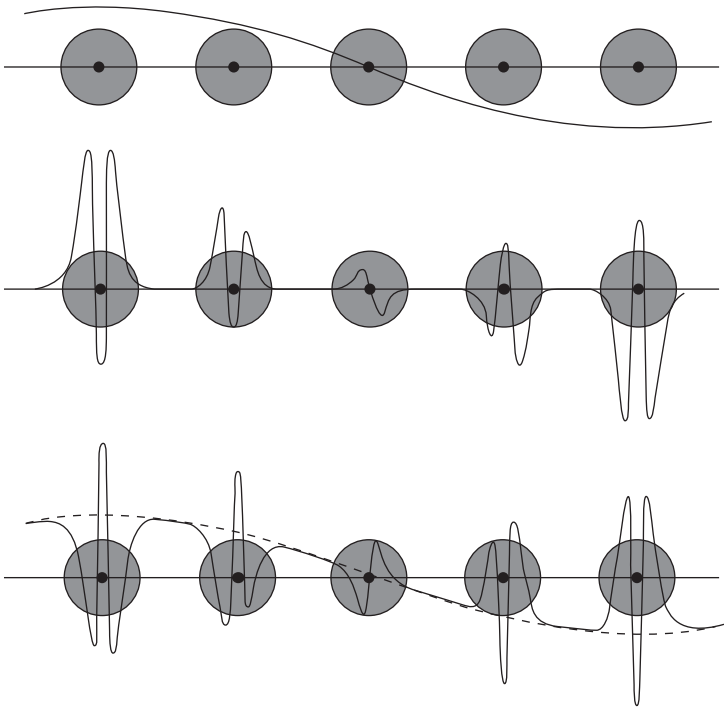

FIGURE 5.15

Plane waves, core functions, and orthogonalized plane waves.

5.7 PSEUDOPOTENTIALS

In 1959, Phillips and Kleinman[14] developed the pseudopotential method that is extensively used to calculate the band structure of metals. This method has been refined through the past 50 years. We will essentially discuss the original theory proposed by Phillips and Kleinman. They showed that advantage can be taken of the crystal symmetry to construct wave functions $\phi_{\mathbf{k}}(\mathbf{r})$, which are smooth parts of the symmetrized Bloch functions. The wave equation satisfied by $\phi_{\mathbf{k}}(\mathbf{r})$ contains an additional term of simple character that corresponds to the usual OPW terms and has a simple physical interpretation as an effective repulsive potential. The sum of the crystal potential and this repulsive potential is known as the pseudopotential. The cancellation between the attractive periodic potential and the repulsive potential in the core region is responsible for the rapid convergence of the OPW calculations for *s* states.

The pseudopotential method starts with the assumption that $\psi_{\mathbf{k}}(\mathbf{r})$, as expressed in Eq. (5.53) and with appropriate coefficients $C_{\mathbf{k}-\mathbf{K}}$ obtained by the use of the variational method, is the exact crystal wave function. We construct a linear combination of the plane waves,

$$\varphi_{\mathbf{k}}(\mathbf{r}) = \sum_{\mathbf{K}} C_{\mathbf{k}-\mathbf{K}} e^{i(\mathbf{k}-\mathbf{K})\cdot\mathbf{r}}, \tag{5.56}$$

which have the same coefficients $C_{\mathbf{k}-\mathbf{K}}$. Because $\psi_{\mathbf{k}}(\mathbf{r})$ must be orthogonal to the core states $\phi_{c\mathbf{k}}(\mathbf{r})$ described in Eq. (5.48), we obtain

$$\psi_{\mathbf{k}}(\mathbf{r}) = \varphi_{\mathbf{k}}(\mathbf{r}) - \sum_c < \phi_{c\mathbf{k}}(\mathbf{r}) \,|\, \varphi_{\mathbf{k}}(\mathbf{r}) > \phi_{c\mathbf{k}}(\mathbf{r}). \tag{5.57}$$

The Schrodinger equation in the crystal is

$$H\psi_{\mathbf{k}}(\mathbf{r}) = \varepsilon_{\mathbf{k}}\psi_{\mathbf{k}}(\mathbf{r}). \tag{5.58}$$

From Eqs. (5.57) and (5.58), we obtain

$$H\varphi_{\mathbf{k}}(\mathbf{r}) - \sum_c < \phi_{c\mathbf{k}}(\mathbf{r}) \,|\, \varphi_{\mathbf{k}}(\mathbf{r}) > H\phi_{c\mathbf{k}}(\mathbf{r}) = \varepsilon_{\mathbf{k}}\varphi_{\mathbf{k}}(\mathbf{r}) - \varepsilon_{\mathbf{k}}\sum_c < \phi_{c\mathbf{k}}(\mathbf{r}) \,|\, \varphi_{\mathbf{k}}(\mathbf{r}) > \phi_{c\mathbf{k}}(\mathbf{r}). \tag{5.59}$$

Using the relation

$$H\phi_{c\mathbf{k}}(\mathbf{r}) = \varepsilon_{c\mathbf{k}}(\mathbf{r})\phi_{c\mathbf{k}}(\mathbf{r}), \tag{5.60}$$

in Eq. (5.59) and rearranging the terms, we obtain

$$H\varphi_{\mathbf{k}}(\mathbf{r}) + \sum_c (\varepsilon_{\mathbf{k}} - \varepsilon_{c\mathbf{k}}) < \phi_{c\mathbf{k}}(\mathbf{r}) \,|\, \varphi_{\mathbf{k}}(\mathbf{r}) > \phi_{c\mathbf{k}}(\mathbf{r}) = \varepsilon_{\mathbf{k}}\varphi_{\mathbf{k}}(\mathbf{r}). \tag{5.61}$$

Eq. (5.61) can be expressed as

$$(H + V_R)\varphi_{\mathbf{k}}(\mathbf{r}) = \varepsilon_{\mathbf{k}}\varphi_{\mathbf{k}}(\mathbf{r}), \tag{5.62}$$

where V_R is the repulsive part of the potential,

$$V_R\varphi_{\mathbf{k}}(\mathbf{r}) \equiv \sum_c (\varepsilon_{\mathbf{k}} - \varepsilon_{c\mathbf{k}}) < \phi_{c\mathbf{k}}(\mathbf{r}) \,|\, \varphi_{\mathbf{k}}(\mathbf{r}) > \phi_{c\mathbf{k}}(\mathbf{r}). \tag{5.63}$$

Thus, Eq. (5.62) is an effective Schrodinger equation satisfied by $\varphi_{\mathbf{k}}(\mathbf{r})$, which is the smooth part of the Bloch function. Because

$$H + V_R = -\frac{\hbar^2}{2m}\nabla^2 + V(\mathbf{r}) + V_R, \tag{5.64}$$

the pseudopotential is defined as

$$V_{ps} = V(\mathbf{r}) + V_R. \tag{5.65}$$

From Eqs. (5.62), (5.64), and (5.65), we obtain

$$H_{ps}\varphi_{\mathbf{k}}(\mathbf{r}) = \left(-\frac{\hbar^2}{2m}\nabla^2 + V_{ps}\right)\varphi_{\mathbf{k}}(\mathbf{r}) = \varepsilon_{\mathbf{k}}\varphi_{\mathbf{k}}(\mathbf{r}). \tag{5.66}$$

The "smoothed" wave function $\varphi_{\mathbf{k}}(\mathbf{r})$ is often referred to as the pseudo wave function that satisfies the effective Schrodinger equation, which has a pseudo-Hamiltonian H_{ps} in which the potential

is relatively small because the pseudopotential V_{ps} is the sum of the lattice potential and the repulsive potential V_R. However, we note from Eq. (5.63) that V_R is a nonlocal operator. Thus, we define

$$V_R(\mathbf{r}, \mathbf{r}') = \sum_c (\varepsilon_{\mathbf{k}} - \varepsilon_{c\mathbf{k}}) \phi_{c\mathbf{k}}(\mathbf{r}) \phi^*_{c\mathbf{k}}(\mathbf{r}') \tag{5.67}$$

such that

$$V_R \varphi_{\mathbf{k}}(\mathbf{r}) = \int V_R(\mathbf{r}, \mathbf{r}') \varphi_{\mathbf{k}}(\mathbf{r}') d\mathbf{r}'. \tag{5.68}$$

Thus, V_R is different when it operates on different functions with different angular momentum. This implies that the effect of the pseudopotential V_{ps} on a wave function is not just to multiply it by a function of $\mathbf{r}$. Further, because V_{ps} depends on the energy $\varepsilon_{\mathbf{k}}$ that is supposed to be the quantity being calculated, one cannot apply some of the basic theorems of quantum mechanics. For example, one cannot apply the theorem that the eigenfunctions belonging to different eigenvalues of H_{ps} are orthogonal.

The pseudopotential formulation has another problem in the sense that there is no unique method to construct the pseudopotential. One can easily show (Problem 5.9) that the valence eigenvalues of the Hamiltonian $H + V_R$ are the same for any operator of the form

$$V_R \varphi_{\mathbf{k}}(\mathbf{r}) = \sum_c < \theta_{c\mathbf{k}}(\mathbf{r}) \,|\, \varphi_{\mathbf{k}}(\mathbf{r}) > \phi_{c\mathbf{k}}(\mathbf{r}), \tag{5.69}$$

where $\theta_{c\mathbf{k}}(\mathbf{r})$ are arbitrary functions. This is also an advantage because one can appropriately choose the functions $\theta_{c\mathbf{k}}(\mathbf{r})$ such that there is good cancellation between $V(\mathbf{r})$ and V_R such that the pseudopotential is small.

As an example, consider

$$\theta_{c\mathbf{k}}(\mathbf{r}) = -V(\mathbf{r}) \phi_{c\mathbf{k}}(\mathbf{r}). \tag{5.70}$$

From Eqs. (5.65), (5.69), and (5.70), we obtain

$$V_{ps} \varphi_{\mathbf{k}}(\mathbf{r}) = V(\mathbf{r}) \varphi_{\mathbf{k}}(\mathbf{r}) - \sum_c < \phi_{c\mathbf{k}} \,|\, V(\mathbf{r}) \,|\, \varphi_{\mathbf{k}}(\mathbf{r}) > \phi_{c\mathbf{k}}(\mathbf{r}). \tag{5.71}$$

Thus, one can subtract from $V(\mathbf{r})$ any sum of the core functions. This cancellation is at the core of the pseudopotential theory because it explains why the valence electrons in metals and semiconductors appear not to interact strongly with the ions of the crystal lattice. The success of the nearly free electron model is a consequence of the cancellation principle implicitly included in the pseudopotential concept. There has been significant improvement in the application of the pseudopotential theory in the band calculations in metals, but here we have essentially discussed the original theory developed by Phillips and Kleinman.

5.8 MUFFIN-TIN POTENTIAL

The muffin-tin potential is a very convenient description of the metal in the sense that it represents an isolated ion within a sphere of radius r_i about each lattice point and constant (zero) everywhere else. Therefore, the periodic potential in the metals considered as a muffin-tin potential is shown in Figure 5.16.

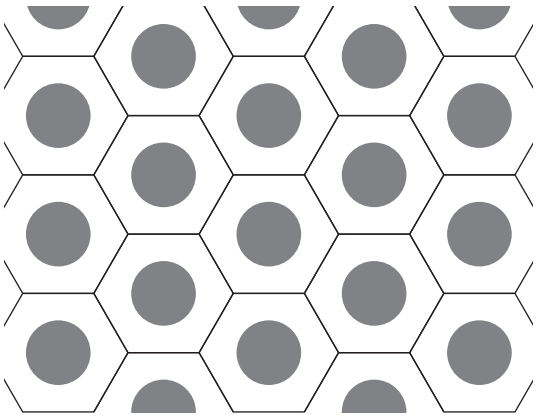

FIGURE 5.16

Muffin-tin potential.

The muffin-tin potential $U(\mathbf{r})$ is considered to be a constant (zero) in the interstitial region and spherically symmetrical within radius r_i about each ion (the core or the atomic region). We assume that there is one ion located at the center of each Wigner–Seitz cell and the spheres do not overlap; i.e., the radius r_i of the sphere is smaller than the Wigner–Seitz radius r_s. Thus, the periodic potential of the lattice can be defined as

$$V(\mathbf{r}) = \sum_i U(|\,\mathbf{r} - \mathbf{R}_i\,|). \tag{5.72}$$

The Schrodinger equation can be solved exactly within each sphere because of the spherical symmetry as well as in the interstitial region where the potential is zero. These solutions are matched on the surface of each sphere, and the Schrodinger equation for the crystal is obtained. The basis states $\phi_{\mathbf{k}\varepsilon}(\mathbf{r})$ are defined as follows:

1. $\phi_{\mathbf{k}\varepsilon} = e^{i\mathbf{k}.\mathbf{r}}$ in the interstitial region (outside the muffin hole). We note that because $\phi_{\mathbf{k}\varepsilon}$ is obtained by matching the solutions at the boundaries of the sphere, there is no precondition that $\varepsilon = \frac{\hbar^2 k^2}{2m}$.
2. In the spherical region about $\mathbf{R}_i$, $\phi_{\mathbf{k}\varepsilon}$ satisfies the atomic Schrodinger equation

$$-\frac{\hbar^2}{2m}\nabla^2\phi_{\mathbf{k}\varepsilon}(\mathbf{r}) + U(\,|\,\mathbf{r} - \mathbf{R}_i\,|\,)\phi_{\mathbf{k}\varepsilon}(\mathbf{r}) = \varepsilon\phi_{\mathbf{k}\varepsilon}(\mathbf{r}),\ |\,\mathbf{r} - \mathbf{R}_i\,| < r_i. \tag{5.73}$$

3. $\phi_{\mathbf{k}\varepsilon}$ is continuous at the boundary of the sphere. There are two elegant methods to solve the eigenvalue problem of this type of Schrodinger equation: the augmented plane-wave (APW) method and the Green's function (KKR) method proposed independently by Korringa, and Kohn and Rostoker (Ref. 11). We will first describe the APW method.

5.9 AUGMENTED PLANE-WAVE (APW) METHOD

The augmented plane-wave (APW) method was proposed by Slater[15]. The potential $U(|\,\mathbf{r} - R_i\,|)$ is a spherically symmetric function within the sphere (muffin-tin hole), and therefore, we write it as $U(\mathbf{r})$. We express the solutions $\psi_\varepsilon(\mathbf{r}) = R_{\varepsilon l}(r)Y_{lm}(\hat{r})$ of an electron in a spherically symmetric potential (note that the energy quantum number is written as ε instead of n and the spherical harmonics $Y_{l,m}(\theta,\phi)$ are expressed as $Y_{l\cdot m}(\hat{r})$). From atomic physics, we know that the radial part of the Schrodinger equation for an atom satisfies

$$-\frac{\hbar^2}{2mr^2}\frac{\partial}{\partial r}r^2\frac{\partial}{\partial r}R_{\varepsilon l}(r) + \left[U(r) + \frac{l(l+1)\hbar^2}{2mr^2}\right]R_{\varepsilon l}(r) = \varepsilon R_{\varepsilon l}(r). \tag{5.74}$$

Ignoring the solution of Eq. (5.74) that diverges at the origin, one can rewrite Eq. (5.73) as

$$\phi_{\mathbf{k}\varepsilon} = \sum_{l=0}^{\infty} \sum_{m=-l}^{l} B_{lm}(k) Y_{lm}(\hat{r}) R_{\varepsilon l}(r). \tag{5.75}$$

The coefficients $B_{lm}(k)$ are arbitrary, which are obtained from the boundary condition that the wave function is continuous across the boundary of each sphere (muffin hole). The wave function in the interstitial is a plane wave $e^{i\mathbf{k}\cdot\mathbf{r}}$. It is well known that the plane wave can be expanded in terms of the spherical harmonics,

$$e^{i\mathbf{k}\cdot\mathbf{r}} = 4\pi \sum_{l=0}^{\infty} \sum_{m=-l}^{l} i^l j_l(kr) Y^*_{lm}(\hat{k}) Y_{lm}(\hat{r}), \tag{5.76}$$

where $j_l(kr)$ is the spherical Bessel function. At the boundary of each sphere, $r = R_i$, where R_i is the radius of each sphere. Matching Eqs. (5.75) and (5.76) at the surface of each sphere where $r = R_i$, we obtain

$$B_{lm}(k) = 4\pi \frac{i^l j_l(kR_i) Y^*_{lm}(\hat{k})}{R_{\varepsilon l}(R_i)}. \tag{5.77}$$

From Eqs. (5.75) and (5.77), we obtain

$$\phi_{\mathbf{k}\varepsilon}(\mathbf{r}) = 4\pi \sum_{l=0}^{\infty} \sum_{m=-l}^{l} \frac{i^l j_l(kR_i) Y^*_{lm}(\hat{k})}{R_{\varepsilon l}(R_i)} Y_{lm}(\hat{r}) R_{\varepsilon l}(r). \tag{5.78}$$

We have a function $\phi_{\mathbf{k}\varepsilon}(\mathbf{r})$ for each value of $\mathbf{k}$ and ε. These APW functions have a discontinuity in slope at the boundary of the muffin tin. The boundary conditions at the edge of the primitive cell can be matched (Problem 5.7) by noting that the APW functions are plane waves at the edge of the primitive cell. The plane waves obey the Bloch condition. Therefore, one can write the solution of the Schrodinger equation of the crystal by making a linear combination of the APWs, all of the same energy ε:

$$\psi_{\mathbf{k}}(\mathbf{r}) = \sum_{\mathbf{K}} b_{\mathbf{k}+\mathbf{K}} \phi_{\mathbf{k}+\mathbf{K}, \varepsilon(\mathbf{k})}(\mathbf{r}), \tag{5.79}$$

where the coefficients $b_{\mathbf{k}+\mathbf{K}}$ are to be determined. The best way is to use the variational principle (Problem 5.8), which is briefly described here.

We define an energy functional,

$$E[\psi] = \frac{\int \left(\frac{\hbar^2}{2m} |\nabla \psi(\mathbf{r})|^2 + V(\mathbf{r}) |\psi(\mathbf{r})|^2 \right) d\mathbf{r}}{\int |\psi(\mathbf{r})|^2 d\mathbf{r}}. \tag{5.80}$$

In the variational technique (Problem 5.8), $E[\psi] = E[\psi_{\mathbf{k}}] = \varepsilon(\mathbf{k})$ when Eq. (5.80) is stationary with respect to a differentiable function $\psi(\mathbf{r})$ that satisfies the Bloch condition with wave vector $\mathbf{k}$. From Eqs. (5.79) and (5.80), one can show that the condition that $E[\psi_{\mathbf{k}}]$ is stationary leads to

$\partial E/\partial b_{\mathbf{k}+\mathbf{K}} = 0$, which yields a set of homogeneous equations in $b_{\mathbf{k}+\mathbf{K}}$. When the determinant of the coefficients of these equations is equal to zero, one obtains an equation of which the roots determine $\varepsilon(\mathbf{k})$.

5.10 GREEN'S FUNCTION (KKR) METHOD

Korringa (1947) and Kohn and Rostoker[11] independently proposed a Green's function method to calculate the band structure of metals. The KKR method essentially uses a Green's function method to solve the Schrodinger equation of a crystalline solid with a periodic potential.

The KKR method starts with the objective to find the "propagating" solutions of the Schrodinger equation in the lattice

$$\left[\frac{-\hbar^2}{2m} + V(\mathbf{r}) - E\right]\psi_{\mathbf{k}}(\mathbf{r}) = 0. \tag{5.81}$$

Here, $V(\mathbf{r})$ is the periodic potential, and the boundary conditions in the central polyhedron (Wigner–Seitz cell) that surrounds the origin are

$$\psi_{\mathbf{k}}(\mathbf{r}_1) = e^{i\mathbf{k}\cdot\mathbf{R}}\psi_{\mathbf{k}}(\mathbf{r}) \tag{5.82}$$

and

$$\partial\psi_{\mathbf{k}}(\mathbf{r}_1)/\partial n_1 = -e^{-i\mathbf{k}\cdot\mathbf{R}}\partial\psi_{\mathbf{k}}(\mathbf{r})/\partial n. \tag{5.83}$$

The conjugate points $\mathbf{r}$ and $\mathbf{r}_1$ are defined (see Figure 5.17) as the points on the surface of the polyhedron separated by the lattice translation vector $\mathbf{R}$.

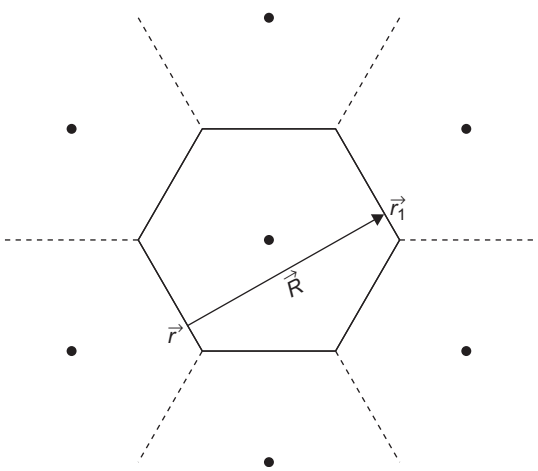

FIGURE 5.17
Conjugate boundary points $\mathbf{r}$ *and* $\mathbf{r}_1$.

The Green's function is defined by

$$\left(\frac{\hbar^2}{2m}\nabla^2 + \varepsilon\right)G_\varepsilon(\mathbf{r}-\mathbf{r}') = \delta(\mathbf{r}-\mathbf{r}'). \tag{5.84}$$

For conjugate boundary points $\mathbf{r}$ and $\mathbf{r}_1$,

$$G_\varepsilon(\mathbf{r}_1-\mathbf{r}') = e^{i\mathbf{k}\cdot\mathbf{R}}G_\varepsilon(\mathbf{r}-\mathbf{r}') \tag{5.85}$$

and

$$\partial G_\varepsilon(\mathbf{r}_1-\mathbf{r}')/\partial n_1 = -e^{i\mathbf{k}\cdot\mathbf{R}}\partial G_\varepsilon(\mathbf{r}-\mathbf{r}')/\partial n. \tag{5.86}$$

It can be shown that $G_\varepsilon(\mathbf{r}-\mathbf{r}')$ can be rewritten in the alternate form

$$G_\varepsilon(\mathbf{r}-\mathbf{r}') = -\frac{2m}{\hbar^2}\frac{e^{i\kappa|\mathbf{r}-\mathbf{r}'|}}{4\pi|\mathbf{r}-\mathbf{r}'|}, \tag{5.87}$$

where

$$\kappa = \sqrt{\frac{2m\varepsilon}{\hbar^2}},\ \varepsilon > 0, \tag{5.88}$$

and

$$= i\sqrt{\frac{2m(-\varepsilon)}{\hbar^2}},\ \varepsilon < 0. \tag{5.89}$$

An alternate way of expressing G is obtained by multiplying Eq. (5.81) by $G^*(\mathbf{r}-\mathbf{r}')$ and the complex conjugate of Eq. (5.84) by $\psi_{\mathbf{k}}(\mathbf{r})$, subtracting and integrating over $\mathbf{r}$ in the interior of the polyhedron (Problem 5.10) to obtain

$$\psi_{\mathbf{k}}(\mathbf{r}) = \int d\mathbf{r}' G_{\varepsilon(\mathbf{k})}(\mathbf{r}-\mathbf{r}')V(\mathbf{r}')\psi_{\mathbf{k}}(\mathbf{r}'). \tag{5.90}$$

Consider the muffin-tin potential

$$\begin{aligned} \hat{V}(\mathbf{r}) &= V(r) - V_0,\ r \le r_i \\ &= 0, r > r_i, \end{aligned} \tag{5.91}$$

Here, r_i is the radius of the inscribed sphere, and V_0 is the average value of the constant potential $V(r)$ in the space between the inscribed sphere and the boundary of the polyhedron. Thus, we can write the periodic potential as

$$V(r) = \sum_i \hat{V}(\mathbf{r}-\mathbf{R}_i). \tag{5.92}$$

From Eqs. (5.87), (5.90), and (5.92), we obtain

$$\psi_{\mathbf{k}}(\mathbf{r}) = \sum_i \int G_{\varepsilon(\mathbf{k})}(\mathbf{r}-\mathbf{r}')\hat{V}(\mathbf{r}'-\mathbf{R}_i)\psi_{\mathbf{k}}(\mathbf{r}')d\mathbf{r}'. \tag{5.93}$$

We move the origin such that $\mathbf{r}'' = \mathbf{r}' - \mathbf{R}_i$, and Eq. (5.93) can be rewritten as

$$\psi_{\mathbf{k}}(\mathbf{r}) = \sum_i \int G_{\varepsilon(\mathbf{k})}(\mathbf{r}-\mathbf{r}''-\mathbf{R}_i)\hat{V}(\mathbf{r}'')\psi_{\mathbf{k}}(\mathbf{r}''+\mathbf{R}_i). \tag{5.94}$$

Using the Bloch theorem $\psi_{\mathbf{k}}(\mathbf{r}''+\mathbf{R}) = e^{i\mathbf{k}\cdot\mathbf{R}}\psi_{\mathbf{k}}(\mathbf{r}'')$ and replacing $\mathbf{r}''$ with $\mathbf{r}'$ in Eq. (5.94), we obtain

$$\psi_{\mathbf{k}}(\mathbf{r}) = \int\limits_{r'<r_i-\varepsilon} d\mathbf{r}'\, G^0_{\mathbf{k},\varepsilon(\mathbf{k})}(\mathbf{r}-\mathbf{r}')\hat{V}(\mathbf{r}')\psi_{\mathbf{k}}(\mathbf{r}'), \tag{5.95}$$

where the integration is done over a single cell, and the structural Green function or Greenian is defined as

$$G^0_{\mathbf{k},\varepsilon(\mathbf{k})}(\mathbf{r}-\mathbf{r}') = \sum_i G_{\varepsilon(\mathbf{k})}(\mathbf{r}-\mathbf{r}'-\mathbf{R}_i)e^{i\mathbf{k}\cdot\mathbf{R}_i}. \tag{5.96}$$

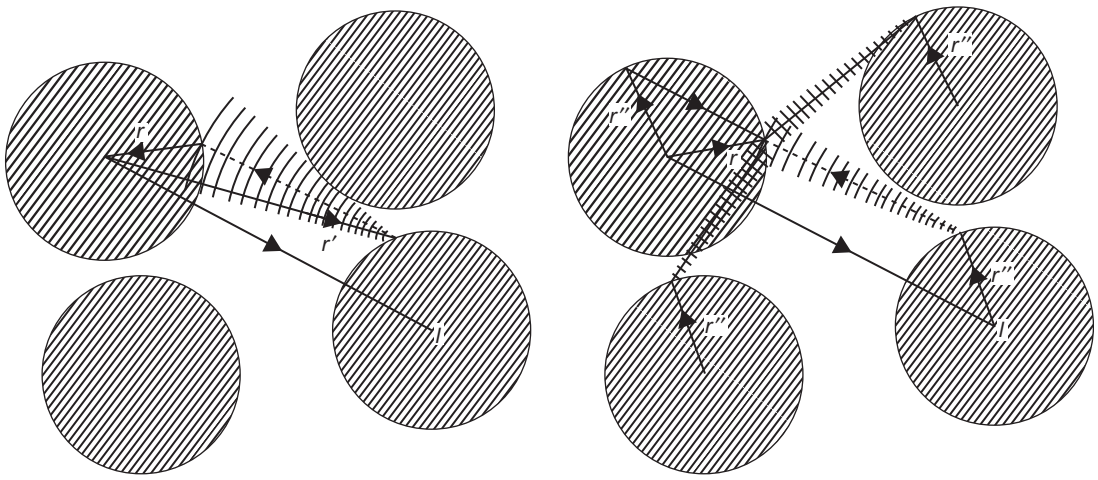

(a) $G(\mathbf{r}-\mathbf{r}')$ propagating from $\mathbf{r}'$ to $\mathbf{r}$

(b) $G^0_{\mathbf{k},\,\varepsilon(\mathbf{k})}(\mathbf{r}-\mathbf{r}')$ combines waves from all points in the lattice.

FIGURE 5.18

(a) The ordinary Green function; (b) the structural Green function.

From Eqs. (5.87) and (5.96), $G^0_{\mathbf{k},\varepsilon(\mathbf{k})}(\mathbf{r}-\mathbf{r}')$ can also be rewritten in the alternate form

$$G^0_{\mathbf{k},\varepsilon(\mathbf{k})}(\mathbf{r}-\mathbf{r}') = -\frac{2m}{\hbar^2}\frac{1}{4\pi}\sum_i \frac{e^{i\kappa|\mathbf{r}-\mathbf{r}'-\mathbf{R}_i|}}{|\mathbf{r}-\mathbf{r}'-\mathbf{R}_i|}e^{i\mathbf{k}\cdot\mathbf{R}_i}. \tag{5.97}$$

The ordinary and structural Green functions are shown in Figure 5.18.

From Eq. (5.96), it can be easily shown that

$$\left(\frac{\hbar^2}{2m}\nabla'^2+\varepsilon\right)G^0_{\mathbf{k},\varepsilon(\mathbf{k})}(\mathbf{r}-\mathbf{r}') = \delta(\mathbf{r}-\mathbf{r}'), \quad r,\, r'<r_i, \tag{5.98}$$

where r_i is the radius of the spherical region in muffin-tin potential. We can also write by using the mathematical identity

$$G^0_{\mathbf{k},\varepsilon(\mathbf{k})}\nabla'^2\psi_{\mathbf{k}}(\mathbf{r}') = \nabla'\cdot(G^0_{\mathbf{k},\varepsilon(\mathbf{k})}\nabla'\psi_{\mathbf{k}}(\mathbf{r}') - \nabla'\psi_{\mathbf{k}}(\mathbf{r}')G^0_{\mathbf{k},\varepsilon(\mathbf{k})}) + \psi_{\mathbf{k}}(\mathbf{r}')\nabla'^2 G_{\mathbf{k},\varepsilon(\mathbf{k})}. \tag{5.99}$$

From Eqs. (5.95), (5.98), and (5.99), we can show that

$$\int_{r'-\varepsilon} d\mathbf{r}'\,\nabla'\cdot[G^0_{\mathbf{k},\varepsilon(\mathbf{k})}(\mathbf{r}-\mathbf{r}')\nabla'\psi_{\mathbf{k}}(\mathbf{r}') - \psi_{\mathbf{k}}(\mathbf{r}')\nabla' G^0_{\mathbf{k},\varepsilon(\mathbf{k})}(\mathbf{r}-\mathbf{r}')] = 0. \tag{5.100}$$

Using the Gauss theorem to transform the volume integral to a surface integral over the sphere of radius $r_i - \varepsilon$, we obtain

$$\int_{r'-\varepsilon} ds' \left[G^0_{\mathbf{k},\varepsilon(\mathbf{k})}(r_i\theta\phi, r_i\theta'\phi') \frac{\partial}{\partial r'} \psi_{\mathbf{k}}(r'\theta'\phi') \mid_{r'=r_i} - \psi_{\mathbf{k}}(r_i\theta'\phi') \frac{\partial}{\partial r'} G_{\mathbf{k},\varepsilon(\mathbf{k})}(r_i\theta\phi, r'\theta'\phi') \mid_{r'=r_i} \right] = 0. \tag{5.101}$$

It can be easily shown[11] that for

$$r < r' < r_i,$$

$$\psi(\mathbf{r}) = \sum_{l=0}^{\infty} \sum_{m=-l}^{m=l} C_{lm} R_l(r) Y_{lm}(\theta, \phi), \tag{5.102}$$

and

$$G^o_{\mathbf{k},\varepsilon(\mathbf{k})}(\mathbf{r} - \mathbf{r}') = \sum_{l,m} \sum_{l',m'} [A_{lm,l'm'} j_l(\kappa r) j_{l'}(\kappa r') + \kappa \delta_{ll'} \delta_{mm'} j_l(\kappa r) n_l(\kappa r')] Y_{lm}(\theta, \phi) Y^*_{l'm'}(\theta', \phi'). \tag{5.103}$$

Here,

$$\begin{aligned} j_l(x) &= (\pi/2x)^{1/2} J_{l+1/2}(x) \\ n_l(x) &= (\pi/2x)^{1/2} J_{-l-1/2}(x), \end{aligned} \tag{5.104}$$

$J_\nu(x)$ are the Bessel functions, and $A_{lm;l'm'}$ are functions of $\mathbf{k}$ and ε, which are characteristics for the lattice under consideration. Substituting Eqs. (5.102) and (5.103) in Eq. (5.101), multiplying by $Y^*_{lm}(\theta, \phi)$, integrating over the sphere $r = r_i - \in$, using the normalization condition $R_l(r_i) = 1$, and finally letting $\in \to 0$, we obtain

$$\sum_{l',m'} j_l [A_{lm;l'm'}(j_{l'} L_{l'} - j'_{l'}) + \kappa \delta_{ll'} \delta_{mm'}(n_{l'} L_{l'} - n'_{l'})] C_{l'm'} = 0, \tag{5.105}$$

where

$$\begin{aligned} L_l &= \frac{dR_l(r)}{dr} / R_l(r) \mid_{r=r_i} \\ j'_l &= \frac{dj_l(\kappa r)}{dr} \mid_{r=r_i} \\ n'_l &= \frac{dn_l(\kappa r)}{dr} \mid_{r=r_i}. \end{aligned} \tag{5.106}$$

Before equating the determinant of Eq. (5.105) to zero, we divide each row by j_l and each column by $(j_{l'} L_{l'} - j'_{l'})$ and obtain the secular equation

$$Det \left| A_{lm;l'm'} + \kappa \delta_{ll'} \delta_{mm'} \frac{(n_l L_l - n'_l)}{(j_l L_l - j'_l)} \right| = 0. \tag{5.107}$$

Eq. (5.107) is used by first tabulating the structure constants $A_{lm,l'm'}$ as functions of ε and $\mathbf{k}$ for each type of lattice. The logarithmic derivatives L_l for the first few l are obtained as functions of energy. The convenient way of solving Eq. (5.107) is to fix ε (and hence κ) to find those $\mathbf{k}$'s ($\mathbf{k}$ enters through the A's) that make Eq. (5.107) vanish. It may be noted that the same expression (Eq. 5.107) can be also obtained by using a variational method.

One may note a good deal of similarity between the Green function (KKR) and the APW method. In the APW method, the expansion is in terms of spherical harmonics. Then a secular determinant is solved for contributions from different lattice vectors. In contrast, in the KKR method, the summation is over lattice vectors (in practice, the summation is over reciprocal lattice vectors by first making a Fourier transformation of $G^0_{\mathbf{k},\varepsilon(\mathbf{k})}(\mathbf{r}-\mathbf{r}')$) and then have a secular determinant in the contributions from different spherical harmonics. Anderson (Ref. 1) has proposed an approximate first-principle method for calculating the band structure of closely-packed structures. In his atomic sphere model (ASM), the atomic polyhedra are replaced by spheres of the same volume and the potential is spherically symmetric within each sphere. The ASM model has no interstitial region.

5.11 MODEL PSEUDOPOTENTIALS

It is obvious from the preceding discussions that the APW and KKR methods do not depend on the atomic potentials, but only on the gradient of R_l at the surface of the atomic sphere. It can be shown from the partial wave theory of scattering that for a spherical potential, the radial solution $R_l(r,\varepsilon)$ can be matched to a free electron wave of the same energy $\varepsilon = \hbar^2\kappa^2/2m$ and angular momentum l, through a phase shift $\eta_l(\varepsilon)$ defined by

$$L_l \equiv \frac{R_l'(R_i,\varepsilon)}{R_l(R_i,\varepsilon)} = \frac{j_l'(\kappa r) - \tan\eta_l(\varepsilon)\cdot n_l'(\kappa r)}{j_l(\kappa r) - \tan\eta_l(\varepsilon)\cdot n_l(\kappa r)}\Big|_{r=R_i}, \tag{5.108}$$

where R_i for a muffin-tin potential is defined in Eq. (5.73) and the spherical Bessel functions and their derivatives were defined earlier. In the model pseudopotential approach, each atomic potential v_a is replaced by a weak potential w_a, which has the same scattering amplitude as conduction electrons. The energy $\varepsilon(\mathbf{k})$ of the crystal would be identical to this hypothetical material. Figure 5.19 shows how the model potential w, with wave function ϕ inside the atom, replaces the effect of the true potential V with the true wave function ψ.

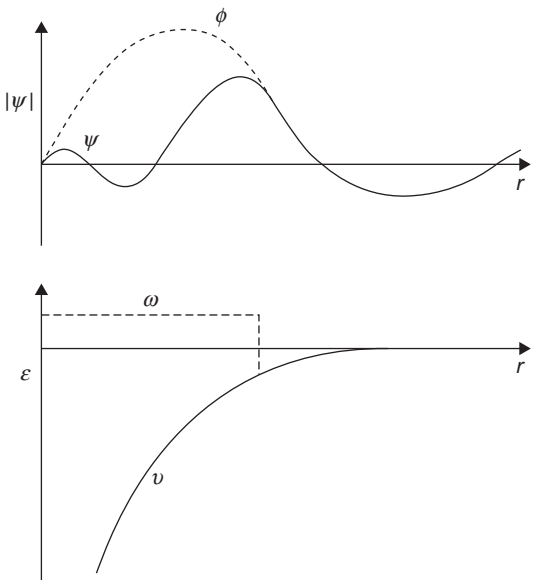

FIGURE 5.19

The true potential V with wave function ψ is replaced by model potential w with wave function ϕ inside the atom.

The analytical pseudopotentials of Phillips and Kleinman are nonlocal, energy dependent, and arbitrary. Thus, one can obtain an infinitely

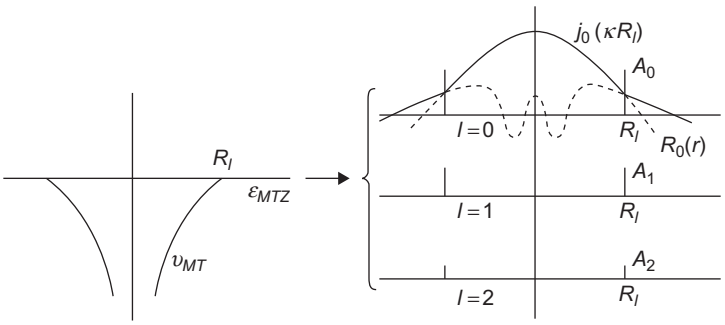

FIGURE 5.20

Model pseudopotential for KKR matrix elements.

large number of localized potentials, $w_l(r,\varepsilon)$, that can be used to obtain the true radial functions R_l outside the atomic core. However, the same model potential $w_l(r,\varepsilon)$ would not work for a different ε or l. Thus, the various angular momentum components in a wave function have to be separated by introduction of appropriate operators. However, it is more convenient to introduce the functional form of each model pseudopotential $w_l(\mathbf{r},\varepsilon)$ for computational convenience. The appropriate choice for a muffin-tin lattice is a delta-function singularity for each value of l, to reproduce the scattering phase shift $\eta_l(\varepsilon)$ at the surface of the sphere.

The model pseudopotential for the KKR matrix elements is shown in Figure 5.20.

It can be shown, by the use of the analytical properties of spherical Bessel functions and plane waves, that the pseudopotential matrix elements used in the KKR method can be written as

$$V_{ps}^{KKR}(\mathbf{K},\mathbf{K}') = -\frac{4\pi N}{\kappa}\sum_l (2l+1)\tan\eta_l' \frac{j_l(|\mathbf{k}-\mathbf{K}|R_i) j_l(|\mathbf{k}-\mathbf{K}'|R_i)}{[j_l(\kappa R_{i)})]^2} P_l(\cos\theta_{\mathbf{KK}'}), \tag{5.109}$$

where

$$\cot\eta_l' \equiv \cot\eta_l - n_l(\kappa R_i)/j_l(\kappa R_i). \tag{5.110}$$

5.12 EMPIRICAL PSEUDOPOTENTIALS

The pseudopotential theory of Phillips and Kleinman established the existence of weak potentials due to cancellations. The empirical pseudopotential concept is based on the assumption that one can choose weak potentials to match the important features of experimental results. An example of the empirical pseudopotential is the empty-core potential. The Ashcroft pseudopotential $U(r)$ is obtained from the approximation that

$$U(r) = 0, \quad r < R_c, \tag{5.111}$$

and

$$U(r) = -U_0 e^{-r/d}/r, \quad r > R_c, \tag{5.112}$$

where R_c is a cutoff radius, and d is the exponential decay length. The Ashcroft (Ref. 2) empty-core pseudopotential is shown in Figure 5.21.

The three parameters in the empty-core pseudopotential are $U_0, R_c,$ and d. These parameters are adjusted to fit the measurement of magnetic or optical experimental results. In general, these types of potentials yield satisfactory results for alkali metals or aluminum.

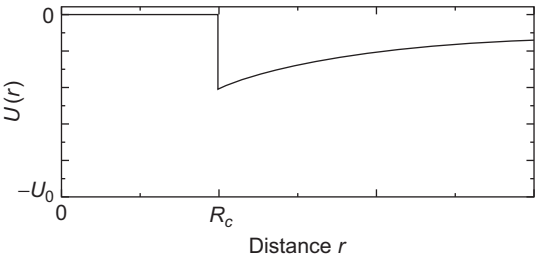

FIGURE 5.21

The Ashcroft empty-core pseudopotential.

5.13 FIRST-PRINCIPLES PSEUDOPOTENTIALS

The starting point for a convenient method of obtaining first-principles pseudopotentials (probably a misnomer) is to start with the Kohn–Sham equations[12] obtained by using the local density approximation (LDA),

$$-\frac{\hbar^2}{2m}\nabla^2\psi_i(\mathbf{r}) + \left[V(\mathbf{r}) + \int d\mathbf{r}'\,\frac{e^2 n(\mathbf{r}')}{|\mathbf{r}-\mathbf{r}'|} + \frac{\delta\varepsilon_{xc}(n)}{\delta n}\right]\psi_i(\mathbf{r}) = \varepsilon_l\psi_i(\mathbf{r}), \tag{5.113}$$

where $\psi_i(\mathbf{r})$ is one of N single-electron wave functions, $n(\mathbf{r})$ is the density defined by

$$n(\mathbf{r}) = \sum_{i=1}^{N} |\psi_i(\mathbf{r})|^2, \tag{5.114}$$

and ε_{xc} is the exchange-correlation energy of the uniform electron gas, which means that it can be chosen freely to ensure that properties of the uniform electron gas are obtained correctly. In the first-principle pseudopotential method, one chooses an atom and makes the approximation that $n(\mathbf{r})$ is spherically symmetric about the nucleus. Thus, the atomic potential is $V(\mathbf{r}) = -\frac{Ze^2}{|r|}$, and all the solutions are of the form $\psi(\mathbf{r}) = R_{nl}(r)Y_{lm}(\theta,\varphi)$, where $R_{nl}(r)$ is the radial wave function and $Y_{lm}(\theta,\varphi)$ is a spherical harmonic. With these approximations, Eq. (5.113) can be rewritten as

$$-\frac{\hbar^2}{2m}\left[\frac{1}{r}\frac{\partial^2}{\partial r^2}r - \frac{l(l+1)}{r^2}\right]R_{nl}(r) + \left[\int \frac{e^2 n(\mathbf{r})}{|\mathbf{r}-\mathbf{r}'|}d\mathbf{r}' - \frac{Ze^2}{r} + \frac{\delta\varepsilon_{xc}}{\delta n} - \varepsilon_{ni}\right]R_{nl}(r) = 0. \tag{5.115}$$

Eq. (5.115) is solved for all the electrons of the atom, and the energies of these states are ε_{ni}.

The outermost states that are in partially filled shells are singled out for special treatment because they contribute to the bonding between atoms and solids. The radial wave functions and the pseudo radial wave functions of such a solid are schematically shown in Figure 5.22.

The radial wave functions for a solid with partially filled shells can be obtained from Eq. (5.115) by using the appropriate values for $n(\mathbf{r})$, Z, ε_{xc}, and ε_{ni}. The corresponding pseudo radial function $R_{nl}^{ps}(r)$ is obtained from each radial function $R_{nl}(r)$ by picking a point beyond the rightmost node and drawing a smooth curve into the origin. This pseudo radial function $R_{nl}^{ps}(r)$

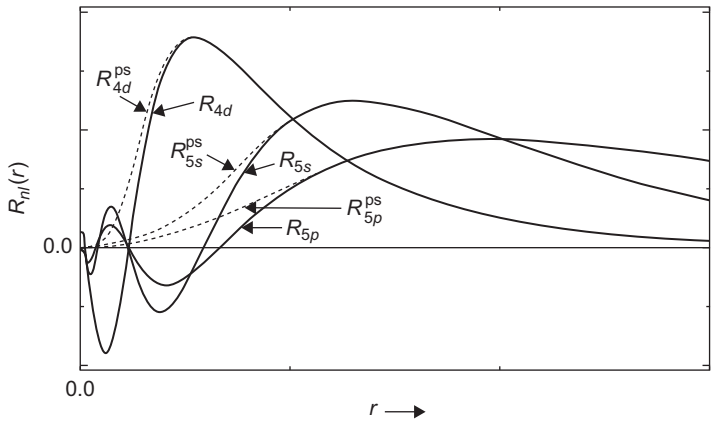

FIGURE 5.22

Schematic diagram of the radial wave functions $R_{nl}(r)$ and pseudo radial wave functions $R^{ps}_{nl}(r)$ for 4*d*, 5*s*, and 5*p* states of a solid with partially filled shells.

should join on to the actual radial function $R_{nl}(r)$ with two continuous derivatives, should be without any nodes, but vanish as r^l at the origin. In addition, the pseudo wave functions built from these pseudo radial functions have to be normalized.

We can now replace the Coulomb potential $-\frac{ze^2}{r}$ in Eq. (5.115) with the pseudopotential

$$V^{ps}_l(r) = \frac{\hbar^2}{2m}\left[\frac{1}{r'R^{ps}_{nl}}\frac{\partial^2 r'R^{ps}_{nl}}{\partial r^2} - \frac{l(l+1)}{r^2}\right] - \left[\int \frac{e^2 n^{ps}(\mathbf{r}')}{|\mathbf{r}-\mathbf{r}'|}d\mathbf{r}' + \frac{\delta\varepsilon_{xc}}{\delta n^{ps}} - \varepsilon_{nl}\right], \tag{5.116}$$

such that when one solves the Kohn–Sham equations, the radial functions R^{ps} are obtained instead of R. However, there is a different $V^{ps}_l(r)$ for each angular momentum state. To be able to resolve this problem that the pseudopotential is nonlocal, we write an arbitrary wave function as a sum of its angular momentum components,

$$\psi(\mathbf{r}) = \sum_{lm} \psi_{lm}(r) Y_{lm}(\theta,\phi). \tag{5.117}$$

We multiply Eq. (5.117) by $Y^*_{l'm'}(\theta,\phi)$, and integrating over θ and ϕ, we obtain

$$\int d\theta d\phi\, Y^*_{l'm'}(\theta,\phi)\psi(\mathbf{r}) = \sum_{lm}\psi_{lm}(r)\int d\theta d\phi\, Y^*_{l'm'}(\theta,\phi)Y_{lm}(\theta,\phi). \tag{5.118}$$

Using the orthonormality condition of the spherical harmonics,

$$\int d\theta d\phi Y^*_{l'm'}(\theta,\phi)Y_{l,m}(\theta,\phi) = \delta_{l,l'}\delta_{m\cdot m'}, \tag{5.119}$$

we can rewrite Eq. (5.118) as

$$\psi_{lm}(r) = \int d\theta d\phi \, Y^*_{lm}(\theta, \phi)\psi(\mathbf{r}). \tag{5.120}$$

The pseudopotential $V_l^{ps}(r)$ defined in Eq. (5.116) is multiplied by $\psi_{lm}(r)$ defined in Eq. (5.120) in forming the Hamiltonian.

PROBLEMS

5.1. The 12 nearest neighbors of the origin of a fcc crystal are

$$\mathbf{R} = \frac{a}{2}(\pm 1, \pm 1, 0), \ \frac{a}{2}(\pm 1, 0, \pm 1), \ \frac{a}{2}(0, \pm 1, \pm 1). \tag{1}$$

Show that for an *s*-level, of which the wave function depends only on the magnitude **r**,

$$\varepsilon(\mathbf{k}) = \varepsilon_s - \beta - 4\gamma(\cos\frac{1}{2}k_x a \cos\frac{1}{2}k_y a + \cos\frac{1}{2}k_y a \cos\frac{1}{2}k_z a + \cos\frac{1}{2}k_z a \cos\frac{1}{2}k_x a), \tag{2}$$

where

$$\gamma = -\int d\mathbf{r}\, \phi^*(x, y, z)\Delta U(x, y, z)\phi(x - \frac{1}{2}a, y - \frac{1}{2}a, z). \tag{3}$$

Show that in the limit of small *ka*, Eq. (2) can be rewritten as

$$\varepsilon(\mathbf{k}) = \varepsilon_s - \beta - 12\gamma + \gamma k^2 a^2. \tag{4}$$

5.2. Show that the tight-binding expression for energies of an *s*-band in a fcc crystal can be written as

$$\varepsilon = \varepsilon_s - \beta - 4\gamma(1 + 2\cos\mu\pi) \quad \text{along } \Gamma X,$$

where $0 \le \mu \le 1$.

5.3. Show that the Bloch functions of different bands and different **k** are orthonormal, i.e.,

$$\int \psi^*_{m\mathbf{k}'}(\mathbf{r})\psi_{n\mathbf{k}}(\mathbf{r})d\mathbf{r} = \delta_{n,m}\delta_{\mathbf{k},\mathbf{k}'}.$$

5.4. Show that $\sum_{\mathbf{k}} e^{-i\mathbf{k}\cdot(\mathbf{R}_i - \mathbf{R}_j)} = N\delta_{i,j}$, where the summation is over all values of **k** in the first Brillouin zone and $\mathbf{R}_i$ and $\mathbf{R}_j$ are direct lattice vectors.

5.5. Show that $\sum_{\mathbf{R}_i} e^{-i(\mathbf{k}-\mathbf{k}')\cdot\mathbf{R}_i} = N\delta_{\mathbf{k},\mathbf{k}'}$, where the summation is over all the direct lattice vectors $\mathbf{R}_i$.

5.6. Show that for a simple cubic lattice of side **a**, the Wannier function at the origin is

$$w_n(\mathbf{r}) = \sqrt{N} u_{n\mathbf{k}}(\mathbf{r}) \frac{\sin(\pi x/a)\sin(\pi y/a)\sin(\pi z/a)}{(\pi x/a)(\pi y/a)(\pi z/a)}, \tag{1}$$

where $u_{n\mathbf{k}}(\mathbf{r})$ is the periodic part of the Bloch function.

5.7. The periodic part of the Bloch function has the property

$$u_{\mathbf{k}}(\mathbf{r}) = u_{\mathbf{k}}(\mathbf{r}+\mathbf{R}), \tag{1}$$

where $\mathbf{R}$ is a Bravais lattice vector. If $\mathbf{r}$ lies on the boundary of the unit cell and $\mathbf{r}+\mathbf{R}$ is another boundary point of the cell, then

$$\hat{n}(\mathbf{r}) \cdot \nabla u_{\mathbf{k}}(\mathbf{r}) = -\hat{n}(\mathbf{r}+\mathbf{R}) \cdot \nabla u_{\mathbf{k}}(\mathbf{r}+\mathbf{R}), \tag{2}$$

where $\hat{n}(\mathbf{r})$ is normal to the cell boundary. Because

$$\psi_{\mathbf{k}}(\mathbf{r}) = e^{i\mathbf{k}\cdot\mathbf{r}} u_{\mathbf{k}}(\mathbf{r}), \tag{3}$$

show that

$$e^{i\mathbf{k}\cdot\mathbf{R}} \hat{n}(\mathbf{r}) \cdot \nabla \psi_{\mathbf{k}}(\mathbf{r}) = -\hat{n}(\mathbf{r}+\mathbf{R}) \cdot \nabla \psi_{\mathbf{k}}(\mathbf{r}+\mathbf{R}). \tag{4}$$

5.8. Define the functional

$$\varepsilon[\phi] = \frac{\int \left(\frac{\hbar^2}{2m} |\nabla \phi(\mathbf{r})|^2 + V(\mathbf{r}) |\phi(\mathbf{r})|^2 \right) d\mathbf{r}}{\int |\phi(\mathbf{r})|^2 d\mathbf{r}}, \tag{1}$$

where

$$\phi(\mathbf{r}) = \psi_{\mathbf{k}}(\mathbf{r}) + \delta\phi(\mathbf{r}). \tag{2}$$

Here, $\psi_{\mathbf{k}}(\mathbf{r})$ is the wave function in the Schrodinger equation,

$$-\frac{\hbar^2}{2m} \nabla^2 \psi_{\mathbf{k}}(\mathbf{r}) + V(\mathbf{r}) \psi_{\mathbf{k}}(\mathbf{r}) = \varepsilon_{\mathbf{k}} \psi_{\mathbf{k}}(\mathbf{r}), \tag{3}$$

$V(\mathbf{r})$ is the periodic potential in the lattice, and both $\phi(\mathbf{r})$ and $\psi_{\mathbf{k}}(\mathbf{r})$ satisfy the Bloch condition. From Eqs. (1) and (2), show that

$$\varepsilon[\phi] = \varepsilon[\psi_{\mathbf{k}}] + O(\delta\phi)^2. \tag{4}$$

Define the functional

$$f[\theta, \varphi] = \int d\mathbf{r} \left(\frac{\hbar^2}{2m} \nabla\theta^* \cdot \nabla\varphi + V(\mathbf{r}) \theta^* \varphi \right). \tag{5}$$

Using the Dirac notation, show that

$$\varepsilon[\phi] = \frac{f[\phi,\phi]}{<\phi\,|\,\phi>}. \tag{6}$$

Using the integration-by-parts formulas for any functions $\varphi_1(\mathbf{r})$ and $\varphi_2(\mathbf{r})$ that have the periodicity of the Bravais lattice,

$$\int_c d\mathbf{r}\,\varphi_1\nabla\varphi_2 = -\int_c d\mathbf{r}\,\varphi_2\nabla\varphi_2 \tag{7}$$

and

$$\int_c d\mathbf{r}\,\varphi_1\nabla^2\varphi_2 = \int_c d\mathbf{r}\,\varphi_2\nabla^2\varphi_1, \tag{8}$$

show that

$$f[\varphi,\psi_{\mathbf{k}}] = \varepsilon_{\mathbf{k}}<\varphi\,|\,\psi_{\mathbf{k}}> \tag{9}$$

and

$$f[\psi_{\mathbf{k}},\varphi] = \varepsilon_{\mathbf{k}}<\psi_{\mathbf{k}}\,|\,\varphi>, \tag{10}$$

where φ also satisfies the Bloch condition. Hence, show that

$$f[\phi,\phi] = \varepsilon_{\mathbf{k}}\{<\psi_{\mathbf{k}}\,|\,\psi_{\mathbf{k}}> + <\psi_{\mathbf{k}}\,|\,\delta\phi> + <\delta\phi\,|\,\psi_{\mathbf{k}}>\} + o(\delta\phi)^2, \tag{11}$$

$$<\phi\,|\,\phi> = <\psi_{\mathbf{k}}\,|\,\psi_{\mathbf{k}}> + <\psi_{\mathbf{k}}\,|\,\delta\phi> + <\delta\phi\,|\,\psi_{\mathbf{k}}> + o(\delta\phi)^2, \tag{12}$$

and

$$\varepsilon[\phi] = \frac{f[\phi,\phi]}{<\phi\,|\,\phi>} = \varepsilon_{\mathbf{k}} + O(\delta\phi)^2. \tag{13}$$

5.9. Show that the valence eigenvalues of the Hamiltonian $H + V_R$ are the same for any operator of the form

$$V_R\varphi_{\mathrm{k}}(\mathbf{r}) = \sum_c <\theta_{c\mathbf{k}}(\mathbf{r})\,|\,\varphi_{\mathbf{k}}(\mathbf{r})>\phi_{c\mathbf{k}}(\mathbf{r}), \tag{1}$$

where $\theta_{c\mathbf{k}}$ are completely arbitrary functions.

5.10. The Schrodinger equation for a crystalline solid with a periodic potential $V(\mathbf{r})$ is

$$\left(\frac{-\hbar^2}{2m}\nabla^2 + V(\mathbf{r}) - \varepsilon\right)\psi(\mathbf{r}) = 0, \tag{1}$$

and the Green's function is defined as

$$\left(-\frac{\hbar^2}{2m}\nabla^2-\varepsilon\right)G(\mathbf{r}-\mathbf{r}')=-\delta(\mathbf{r}-\mathbf{r}'). \tag{2}$$

Multiply Eq. (1) by $G^*(\mathbf{r}-\mathbf{r}')$ and the complex conjugate of Eq. (2) by $\psi(\mathbf{r})$, subtract and integrate over **r,** use the Hermitian property of the Green's function

$$G_\varepsilon(\mathbf{r}-\mathbf{r}')=G_\varepsilon^*(\mathbf{r}'-\mathbf{r}), \tag{3}$$

and show that

$$\psi_{\mathbf{k}}(\mathbf{r})=\int d\mathbf{r}'G_{\varepsilon(\mathbf{k})}(\mathbf{r}-\mathbf{r}')V(\mathbf{r}')\psi_{\mathbf{k}}(\mathbf{r}'). \tag{4}$$

References

1. Anderson OK. Simple approach to the band structure problem. *Solid State Commun* 1973;**13**:133.
2. Ashcroft NW. Electron-ion pseudopotentials in metals. *Phys Lett* 1966;**23**:48.
3. Ashcroft NW, Mermin ND. *Solid state physics*. New York: Brooks/Cole; 1976.
4. Bullett DW. *Solid State Phys: Adv Res Appl* 1982;**35**:129.
5. Callaway JC. *Quantum theory of the solid state*. New York: Academic Press; 1976.
6. Car R, Parrinello M. United approach for molecular dynamics and density functional theory. *Phys Rev Lett* 1985;**55**:2471.
7. Goswami A. *Quantum mechanics*. Dubuque: Wm. C. Brown; 1997.
8. Harrison WA. *Pseudopotentials in the theory of metals*. New York: Benjamin; 1966.
9. Heine V. *Solid State Phys: Adv Res Appl* 1970;**24**:1.
10. Heine V, Wearie D. *Solid State Phys: Adv Res Appl* 1970;**24**:250.
11. Kohn W, Rostoker N. *Phys Rev* 1954;**94**:1111.
12. Kohn W, Sham LJ. Self-consistent equations including exchange and correlation effects. *Phys Rev* 1965;**140**:A1133.
13. Kohn W, Rostoker N. Solution of the Schrodinger equation in periodic lattice with an application to metallic lithium. *Phys Rev* 1954;**94**:1111.
14. Korringa J. On the calculation of the energy of a Bloch wave in a metal. *Physica* 1947;**13**:392.
15. Marder MP. *Condensed Matter Physics*. New York: Brooks/Cole; 2000.
16. Phillips JC, Kleinman L. New Method for calculating wave functions in crystals and molecules. *Phys Rev* 1959;**116**:287.
17. Slater JC. Wave funcions in a periodic potential. *Phys Rev* 1937;**51**:846.
18. Slater JC, Koster GF. Wave functions in a periodic potential. *Phys Rev* 1956;**94**:1498.
19. Wannier GH. *Elements of solid state theory*. Cambridge: Cambridge University Press; 1959.
20. Wigner E, Seitz F. On the constitution of metallic sodium. *Phys Rev* 1933;**43**:804.
21. Wigner E, Seitz F. *Solid State Phys: Adv Res Appl* 1955;**1**:97.
22. Ziman JM. *Principles of the theory of solids*. Cambridge: Cambridge University Press; 1972.